# CLIMATE CHAPTER

This document was developed with the University of South Carolina, South Carolina State Climatology Office and South Carolina Sea Grant Consortium. The chapter includes background information regarding the drivers of global climate and climate variability, long-term changes in South Carolina's instrumental record, and projected future changes in the state.

DRAFT

# Climate Chapter

## Introduction and Scope

This chapter includes an evaluation of historical climate trends and potential future climate change in South Carolina. It begins with background information regarding the drivers of global climate and climate variability, long-term changes in South Carolina's instrumental record, and projected future change in the state. The chapter includes analysis of South Carolina's observed climate record, translation of model output into future state-level climate projections, and synthesis of relevant peer- reviewed research.

## Observations and Projections for South Carolina's Climate

### Global climate change

Global, regional, and local climate varies through time and is influenced by many factors. Changes in solar output, Earth's orbital cycles, volcanic eruptions, and feedbacks within the climate system are often considered "natural" causes of climate change. By contrast, "anthropogenic" factors include those resulting from human activities, such as the emissions of *greenhouse gases*. Today, both natural and anthropogenic factors affect Earth's climate across all scales – both spatial and temporal. In the absence of any changes, the earth-atmosphere system will maintain a radiation balance by which absorbed solar radiation is matched by outgoing infrared radiation (Figure 5.1). Climate scientists often use the concept of *radiative forcing* to quantify changes to this balance. It is possible, for example, to estimate how solar cycles, changes to Earth's axial tilt, emission of aerosols from volcanic eruptions or industrial activity, cloud type and distribution, or land use changes alter the solar radiation absorbed at Earth's surface, or how changing greenhouse gas concentrations affect the rate of radiation loss to space. The increase of greenhouse gas concentrations since the industrial revolution has slowed this latter rate such that absorbed solar radiation exceeds outgoing radiation in the lower atmosphere, causing a radiation imbalance (Loeb et al., 2021). This is an example of what is called *positive* radiative forcing – a net increase in available energy that alters the radiative balance. The climate system adjusts to a new radiative balance by warming the surface and lower atmosphere, which, in turn, causes greater emission of energy to space.

How much have greenhouse gases altered the radiation balance during the industrial period, and what has been the resulting climate response? Global carbon dioxide ($CO_2$) concentrations sampled from ice cores reveal atmospheric levels of approximately 280

parts per million (ppm) in the preindustrial period (pre-1750). Direct measurements since 1958 indicate an increase from 315 ppm to more than 415 ppm in 2022 (National Oceanic and Atmospheric Administration [NOAA], 2022b). Other greenhouse gases such as methane, nitrous oxide, and fluorinated gases have also risen during this period. The positive radiative forcing caused by these well-mixed greenhouse gas increases is large compared to other natural factors. When considering all the major factors altering Earth's *radiation budget* since 1850, it is estimated that human activity has caused a net global effective radiative forcing of approximately 2.75 Watts per square meter ($Wm^{-2}$; Smith et al., 2020). Climate models simulate a global temperature response to changes in natural and anthropogenic forcing since 1850 of approximately 2°F, consistent with the observed temperature increase (Figure 5.2). Climate simulations that exclude this human influence fail to capture the observed temperature increase of the last 60 years.

## Data and methods

The temperature record at a given place reflects global as well as local factors; detecting change requires consistent, long-term monitoring. In South Carolina an observation network established in the late 1800s provides a rich data set to examine historic variability and trends. These data are part of the Global Historical Climatology Network-Daily (GHCN-Daily) quality-controlled dataset with long, reliable records (Menne et al., 2012). GHCN-Daily data provide the basis for aggregated data at the state and climate division level (Vose et al., 2014) and provide the foundation for analysis of temperature and precipitation changes in South Carolina. The National Centers for Environmental Information (NCEI) maintain these data sets and make them freely available. Some analysis is done using fifteen stations from the network. These were selected based on station length, completeness, and spatial distribution and in consultation with the South Carolina State Climatology Office. Most of these stations were used in a brief 2022 state-level climate summary conducted by NCEI (Kunkel et al., 2022). We used a Mann-Kendall Trend Test to determine whether significant trends exist in the temperature and precipitation records of the fifteen select stations using records from approximately 1900 to 2020. We computed Sen's slope to determine a linear rate of temperature and precipitation change.

The degree of future global warming depends on greenhouse gases already emitted and those that will be emitted in future decades. Since future greenhouse gas emissions depend on unknown future energy technology and policies, different emission scenarios are typically considered. In this chapter we will refer to two commonly-used scenarios – as a "lower emissions" scenario (RCP4.5) and a "higher emissions" scenario (RCP8.5). These *representative concentration pathways* (RCPs) are linked to specific stabilized end-of-century radiative forcing of 4.5 and 8.5 Watts per square meter respectively (Moss et al., 2010). Recalling that the radiative forcing from 1850 to 2020 is

approximately 2.75 $Wm^{-2}$, these values represent an additional 1.75 and 5.75 $Wm^{-2}$ by 2100. To provide context, by 2100 the lower emissions (RCP4.5) scenario would lead to a $CO_2$ concentration of approximately 550 ppm (about double the pre-industrial value), and the higher emissions (RCP8.5) scenario would result in $CO_2$ concentration of about 900 ppm (more than triple the pre-industrial value). The higher emissions scenario used here would lead to an end-of-century forcing that is two to three times higher than that witnessed thus far.

The two emissions scenarios serve as inputs to global climate models that simulate Earth's climate response. As seen in Figure 5.2 these models capture well the global temperature trends during historical periods. At a state level, it is important to consider more than one climate model, since they collectively produce a range of plausible changes at this scale. For this study, we examined output from all models considered in the Fifth Coupled Model Intercomparison Project (*CMIP5*; Taylor et al., 2012). Of these, we more closely considered output from nine climate models and, when available, an average from an *ensemble* of all models. The nine-member subset was selected largely based on model performance in the southeastern United States (Engström & Keellings, 2018; Keellings, 2016; Rupp, 2016). From this, we selected "bookends" that capture a wide range of warm, cool, wet, and dry projections for the 21st century. This methodology accounts for the variability and uncertainty associated with state-level projections. Since most GCMs produce output at coarse (50-125 mile) grid cells, state, and regional studies commonly use "*downscaled*" data sets for future climate scenarios. We used statistically-downscaled data from CMIP5 provided by the Localized Constructed Analogs (LOCA; Pierce et al., 2014) data set. LOCA has several advantages for use in this state-level assessment: it was also used in the Fourth National Climate Assessment (Hayhoe et al., 2017) and corrects for regional bias by comparing simulations against observations during the historic period and adjusting output to match general statistical properties. In our examples, climate model output from LOCA was produced using historic greenhouse emissions, 1950-2005, and projected emissions 2005-2100 according to the lower (RCP 4.5) and higher (RCP 8.5) emissions scenarios.

## South Carolina temperature

### Key findings

- Since 1895, average annual temperature has increased by approximately 1°F, lower than the average global increase of approximately 2°F. However, the rise during the past 60 years has matched or exceeded global increases and the past 30 years have been warmer than any other consecutive 30-year period.
- The instrumental temperature record includes considerable year-to-year and decade-to-decade variability.
- Most stations exhibit statistically-significant increases in a) maximum temperature in winter, spring, and summer, and b) minimum temperature in

summer. While the state has had temperature increases in the past sixty years, few stations exhibit maximum temperature trends during fall, or minimum temperature trends during winter, spring, or fall when considering records from the beginning of the early 20th century.

- Climate models project South Carolina temperature increases of 5° to 10°F by the year 2100, depending on future greenhouse gas emissions.

### Observed temperature

State-wide average data provide a snapshot of general temperature trends for the past 125 years (Figure 5.3). The state experienced a relatively warm period from the mid-1920s to the mid-1950s, a cooler period during the next three decades, and an increase since the early 1980s. Average temperature during the past 30 years is warmer than any other consecutive 30-year period in the record. The state's average annual temperature increased by approximately 0.9°F per century. These increases are slightly lower for annual maximum temperature (approximately 0.8°F per century) and slightly higher for annual minimum temperature (approximately 1.0°F per century). South Carolina's average annual temperature pattern is typical of the broader southeastern United States during these past 125 years. Additional comparison with global and national (lower 48 states) patterns reveals at least two key points (Figure 5.4). First, *interannual* and *interdecadal* variability is typically higher at an individual state level than at national or global scales. This is because atmospheric and ocean circulation patterns smooth trends much more at global than regional scales. Second, while South Carolina's average rate of temperature rise from 1895 to 2020 is lower than the average global rate, the 3°F increase in the most recent fifty years is comparable to or even higher than the global average increase.

A selection of South Carolina's most complete GHCN-Daily stations allows us to identify statistically significant temperature trends by season. Like the South Carolina versus global temperature anomalies (Figure 5.4), individual stations often experience higher year-to-year and decade-to-decade variability than spatially-averaged data. Because of this, detecting a statistically significant trend for the entire period requires large changes through time. Many stations do not show such changes, but there are some examples where the changes are dramatic enough to reveal a clear, statistically significant signal. For example, eight of the fifteen long-term and most reliable stations have experienced significant spring maximum temperature increases (Figure 5.5). Five of the stations show significant summer maximum temperature increases at a 99% confidence level (Figure 5.6). Winter maximum temperature increased at all but two stations; it was statistically significant at seven of the fifteen stations (Figure 5.7). Summer minimum temperature increases occurred at ten stations, nine of which were statistically significant (Figure 5.8). Two stations had decreasing trends, significant at the 99% confidence level.

Temperature plots from Little Mountain illustrate how dramatic the changes must be for trends to be statistically significant given the high interannual and interdecadal variability in South Carolina temperature records (Figure 5.9). The bars in the graph show departures from the 1901-1960 spring temperature average, also called *anomalies*. Note that, despite the strong year to year variability, warmer than average temperatures are more frequent in recent decades, with cooler than average temperatures less common.

### Future temperature projections

Climate model simulations capture the average temperature increase seen in South Carolina from 1950 to the early 2000s (Figure 5.10). In the lower emissions scenario, the ensemble average of all models projects an additional increase of 4°F from the 1991-2020 average by 2100; it ranges from an increase of approximately 3°F in a cooler model to 5°F in a warmer model (Figure 5.11). It is important to note that this lower emissions scenario assumes decreasing greenhouse gas emissions in the next decade and leveling $CO_2$ concentrations below 450 ppm by the end of the century. By contrast, the high emissions scenario leads to a much greater temperature increase – projected at 6°F, 8°F, and 10°F during the 21$^{st}$ century for the cooler model, ensemble average, and warmer model respectively (Figure 5.12).

Projected changes in temperature extremes also vary by emissions scenario and individual model. By the end of the century, the number of days in which state-averaged maximum temperature would exceed 95°F doubles in the lower emissions scenario, using output from a cooler model. In the higher emissions scenario with a warmer model, the number increases five-fold. Projections from a model ensemble average show changes in hot days across space and contrasts between emissions scenarios Figures 5.13 and 5.14). Such increases would likely have ecological impacts, as well as implications for human health and cooling costs during the warm season. Warm nights, as measured by state-averaged minimum temperature above 75°F, also increase in future scenarios, from double to six times the number of days per year, depending on emissions scenario and model (Figures 5.15). Meanwhile, cold extremes, in this case defined by number of days in which the state-wide average minimum temperature is cooler than 32°F, drop by half in the high emissions scenario (Figures 5.16).

## South Carolina precipitation

### Key findings

- Precipitation has varied greatly on a yearly and decadal basis.
- Summer precipitation has decreased and the number of precipitation days in fall has increased; overall, few other statistically significant trends are found for seasonal or annual total precipitation.

- There are relatively few statistically significant long-term trends in heavy precipitation. However, recent heavy precipitation events affecting the coastal regions and the Pee Dee River Basin (2015, 2016, 2018) match expectations of a warmer world with higher evaporation rates and atmospheric moisture.
- Drought has periodically affected all parts of the state. The historical record reveals lots of interannual and interdecadal variability, but no statistical trend. Rising temperatures in the 21st century will likely exacerbate agricultural and hydrologic drought.

## Observed precipitation

South Carolina's precipitation varies across years and decades (Figure 5.17), influenced by the paths and frequency of *extratropical cyclones* and *tropical cyclones*, the position of the *sub-tropical high*, and sea-surface temperatures in the Gulf of Mexico and Atlantic (Curtis, 2008; Diem, 2006; Labosier & Quiring, 2013; Qian et al., 2021; Rickenbach et al., 2015). Consequently, there are few statistically significant trends in the annual or seasonal precipitation record. One exception is summer (June, July, August total) precipitation which has decreased at all long-term stations and is statistically significant at two-thirds of these stations, mostly those away from the coast (Figure 5.18).

Data from the Santuck station illustrate the statistically significant decrease of total summer precipitation found at many South Carolina stations (Figure 5.19). The bars in this time series represent the difference of each summer's precipitation from the 1901-1960 average. The Santuck example also shows the considerable variability of precipitation from year to year and decade to decade, common to all South Carolina stations. It is large enough at many stations that long-term monthly or seasonal precipitation changes do not have statistically significant trends relative to this interannual and interdecadal variability. Three exceptions include a decrease in February and an increase in November precipitation totals at all long-term stations (statistically significant at 60-70% of them), and an increase in rain days during fall at most South Carolina stations.

## Future precipitation projections

Most future precipitation projections show modest increases through the 21st century (Figure 5.20). There is a range among even those models with the best performance in the southeastern US during the historic period. One wetter model shows an average increase of about 10% with annual swings exceeding 40% of current average conditions. A drier model shows decreases of 10% and annual swings of 40% lower than current average conditions. The ensemble mean shows state-averaged precipitation increases of 5-10%. It is important to note that even if South Carolina's precipitation increases in the future, some of this increase would be offset by higher evaporation rates caused by warming. Under those conditions it is possible for precipitation to increase, but

moisture availability in soils and watersheds to decrease because of higher evaporation rates. Moisture availability also depends on the nature of precipitation changes. If delivered in shorter, more intense bursts, more precipitation could runoff land surfaces, limiting soil moisture gains.

### Precipitation extremes

Precipitation extremes potentially pose even greater social risks than changes in monthly, seasonal, or annual averages do. South Carolina experiences many heavy precipitation events fueled by moisture delivery from the Gulf of Mexico and Atlantic, as well as lift from thunderstorms, tropical cyclones, and fronts. Changes in either moisture supply or storm patterns can alter the frequency of heavy precipitation events and the intensity, or rate, at which precipitation falls during these events.

Analysis of South Carolina precipitation extremes reveals three fundamental things. First, most measures of heavy precipitation have large interannual and interdecadal variability, even greater than that seen in monthly, seasonal, or annual total precipitation. Second, while heavy precipitation has increased since the mid-1900s at many southeastern US stations (Easterling et al., 2017; Powell & Keim, 2015), the picture is less consistent in South Carolina, where most stations do not exhibit significant long-term trends (Moraglia et al., 2022). Few stations in South Carolina, for example, have significant changes in the 1-day precipitation amounts expected with 50%, 10%, or 1% probability in any given year (often called 2-, 10-, and 100-year events, respectively). The large interannual and interdecadal variability, combined with the infrequency of extreme precipitation events, makes finding statistically significant long-term trends difficult. Third, despite the lack of long-term trends, extreme events during the past decade (including 2015, 2016, and 2018) are among the highest in the historic record and have resulted in extensive property damage and loss of life.

One South Carolina station that does show a long-term, statistically significant increase in heavy precipitation is Conway. Analysis of 50-year periods for the station clearly shows how big events in recent decades have affected 1-day precipitation probabilities. For a given precipitation depth there is a higher probability of occurrence when considering 50-year periods after 1950 versus those earlier in the 20$^{th}$ century (Figure 5.21). For example, a 5-inch rainfall event has a one-in-ten chance of occurring in any given year (the so-called 10-year event) when using 1930-1979 precipitation data, but a one-in-five chance of occurring (a 5-year event) using 1970-2019 data. This has implications for infrastructure designed and built decades ago.

In Conway's case, have recent events altered the precipitation probability of the full record? Specifically, how do probabilities of 1-day precipitation maxima during the period 1910-2000 (used in the widely-referenced *Atlas-14*) differ from those using data

from 1910-2020? Such differences, it turns out, are relatively modest (Figure 5.22). The likely reason is that the 1910-2000 record includes 11.35 inches of precipitation from 1999's Hurricane Floyd, which already shifted the tails of the distribution. Large shifts in probability require unprecedented events, and big events after 1999 have not yielded higher 1-day precipitation at Conway.

Because heavy rainfall frequently occurs for only short durations across small areas, it is often undetected, particularly by the few weather stations with the long, consistent records necessary for evaluating change. Even fewer stations measure hourly precipitation, which may be more important for capturing intensity as highest hourly precipitation can contribute more than 40% of a day's total (Barbero et al., 2019). A recent study of 1960-2015 trends in hourly precipitation at National Weather Service stations in Greenville, Columbia, and Charleston, as well as Wilmington and Charlotte, NC, and Savannah and Augusta, GA (Brown et al., 2019), found significant shortening of storm duration at all stations (90% confidence) and increasing hourly totals at Charleston (95% confidence), and Savannah, Charlotte, and Wilmington (90% confidence). By contrast, the frequency of events exceeding the station-specific average hourly accumulation dropped significantly at three stations — Greenville, Columbia, and Savannah (90% confidence). These mixed results warrant more investigation of sub-daily precipitation records.

Climate change could alter moisture availability and storm systems in ways that affect precipitation intensity. Globally, water vapor increases by approximately 7% for each 1.8°F (1°C) temperature increase (Trenberth et al., 2003). While this relationship does not translate directly to heavier precipitation events, research has documented connections between moisture availability and increases in observed and modeled precipitation intensity at global, continental, and regional scales (Fischer & Knutti, 2016; Forestieri et al., 2018; Grabowski & Prein, 2019; Huang et al., 2017; Kunkel et al., 2020a; Lehmann et al., 2015; O'Gorman & Schneider, 2009; Tabari, 2020). Heavy precipitation events in the southeastern US are strongly driven by precipitable water availability (Kunkel et al., 2020b; Kunkel et al., 2020c). As temperature increases cause higher evaporation rates from the Gulf and Atlantic, delivery of precipitable water to South Carolina should increase in the 21st century. Only significant changes in storm frequency and dynamics would curtail heavier precipitation in the future. Projections from climate models show consistent increases in atmospheric moisture delivery to the Southeast with consequent increases in heavy precipitation at daily to hourly scales (Easterling et al., 2017; Prein et al., 2017).

Current climate models generate plausible global scenarios, but their ability to project daily or hourly precipitation for a specific region is limited. Recent application of statistical methods and high-resolution climate models has helped to quantify the

degree to which individual heavy precipitation events can be blamed on global-scale climate change. Examples of such *attribution* studies exist for a heavy rainfall event due to a stationary low-pressure system near Louisiana (van der Wiel et al., 2017) and for tropical cyclones, including Hurricane Harvey (Patricola and Wehner, 2018; Risser and Wehner, 2018; van Oldenborgh et al., 2017). While many uncertainties remain, new initiatives for more detailed precipitation monitoring and for climate modeling that incorporates convective cloud dynamics should further improve our understanding of how global-scale climate changes can affect heavy short-duration rainfall (Blenkinsop et al., 2018; Fowler et al., 2021).

The recent record of heavy precipitation in the Carolinas provides a tangible example of precipitation extremes, their spatial extent, and the potential for loss of life and property. Precipitation in October 2015, October 2016, and September 2018 produced record rainfall in large parts of eastern and central South Carolina, demonstrating how rare events can happen in quick succession — a compounding hazard that produced repetitive losses across the Pee Dee Basin. In just a few years, events with a 1% annual probability or less occurred multiple times in some locations (Figure 5.23). As reported elsewhere (Jalowska et al., 2021), the three extraordinary events are at the high end of future projections for precipitation intensity. Similar repetitive events have affected North Carolina during the past two decades (Paerl et al., 2019). In many ways, attributing these events to climate change is moot. What we know is that they are consistent with expectations of a warmer world with higher evaporation rates and atmospheric moisture and provide tangible examples of the state's vulnerability to heavy precipitation.

Aside from observed or modelled changes in precipitation intensity, changes to the surface on which precipitation falls can alter the impacts of heavy rainfall events. Most of South Carolina has experienced increases in impervious surfaces in recent decades, a trend that is likely to continue through the 21$^{st}$ century (Terando et al., 2014). For example, urbanization around Charleston has resulted in land use and land cover change five times larger than the rate of population growth since 1990 (Allen & Lu, 2003). This land-use change accelerates the delivery of water to rivers, lakes, and wetlands, increasing the likelihood that a given amount of precipitation will lead to flooding.

### Drought

South Carolina has endured extensive periods of *meteorological*, *agricultural*, and *hydrologic* drought as well as anomalously wet periods. The standardized precipitation index measures the intensity of wet or dry spells by comparing a fixed period against all such periods in the historic record. Historic records of this meteorological drought index show regular cycles of wet and dry periods during the past 125 years. By

incorporating estimates of evapotranspiration, infiltration, and runoff, however, the Palmer hydrological drought index provides a more complete measure of moisture deficit and surplus and is more commonly used when considering impacts on water resources (Figure 5.24). Both measures qualitatively show interannual and interdecadal variability in dry and wet periods, but no obvious historical trends in either. This echoes other recent research showing little statistically significant evidence for changing drought length or intensity in North Carolina (Soulé, 2022). South Carolina has also historically experienced rapid drought onset (i.e., "flash droughts"), and despite its relatively small size, has experienced considerable variability across the state (Figure 5.25).

Projections of future meteorological drought in the state are mixed. Some recent work suggests very modest changes in projected consecutive dry days during the warm season and spatially mixed changes during the cool season (Keellings & Engström, 2019). More generally in the literature, there is relatively low confidence in human influence on meteorological drought because of uncertainties in precipitation projections. There is medium confidence that global climate change could exacerbate agricultural and ecological drought, reflecting greater consensus on temperature increases that cause more evaporation from waterways and soil (Arias et al., 2021). Projections of drought measures that incorporate an evaporation component show a trend towards drier conditions in the Southeast (Ahmadalipour et al., 2017).

## Tropical cyclones

### Key findings

- South Carolina's geographic position makes it vulnerable to tropical cyclones. The impact of tropical storms and hurricanes affecting the state have fluctuated greatly across years and decades.
- Their frequency and intensity have been influenced by large-scale conditions including sea-surface temperature and wind shear.
- Future scenarios are mixed with respect to the frequency of storms, but more consistently project greater intensity of wind and precipitation for those storms that do occur.

### Observed variability

South Carolina's geographic position lends itself to periodic influences of tropical cyclones (i.e., tropical storms and hurricanes; Figure 5.26). Warm waters in the tropical Atlantic foster the development of these storms, that typically travel from east to west in the tropical trade wind belt. The Bermuda High pressure system in the subtropical Atlantic steers these storms when they drift north, sometimes towards South Carolina, bringing high winds, storm surge, and heavy precipitation. Some of these storms make

direct strikes on the state from the Atlantic, others strike nearby states or brush the coast, still others enter as "backdoor" storms moving north from the Gulf of Mexico and ultimately affect South Carolina. Tropical cyclone activity varies greatly from year to year and decade to decade, across the Atlantic Basin and the Gulf of Mexico. This variability is greater still when considering a geographic unit as small as a single state. Activity depends on many variables, particularly sea-surface temperature and wind shear across tropical and subtropical waters. In addition, conditions in the tropical Pacific (associated with El Niño/La Niña cycles) and thunderstorm activity in West Africa both influence the formation and development of Atlantic hurricanes.

### Future projections

Climate change could affect tropical cyclone frequency, intensity, and associated precipitation. Evidence for historic and projected changes come from observational analysis and climate model simulations, respectively. The observational record provides scant evidence for statistically significant changes in the number of North Atlantic hurricanes, though such investigations are hampered by a relatively short observational record (particularly over oceans), and high natural interannual and interdecadal variability. Likewise, future projections for 21st century North Atlantic hurricane frequency are mixed. While some modeling studies have indicated the possibility for fewer tropical cyclones (Mallard et al., 2013), others have shown no significant changes (Jing et al., 2021), or little basis for such decreases (Emanuel, 2021). Moreover, a panel of hurricane experts have expressed low to medium confidence in projections indicating a future decrease in the number of events (Knutson et al., 2020). The necessary conditions for hurricane formation are well-known, but a more complete understanding of actual hurricane genesis is required for consistent and reliable estimates of future frequency (Sobel et al., 2021).

By contrast, observations and models show more consistency regarding recent and projected changes in hurricane intensity (Wu et al., 2022). Estimates during the satellite-era (since 1979) show that category 3 and higher storms have increased in number by 8% per decade (Kossin et al., 2020). Models consistently link increasing tropical cyclone intensity to a warmer world where increasing sea-surface temperatures provide more energy to the storm through increased condensation within its cumulonimbus and cumulus clouds (Emanuel, 2021; Jing & Lin, 2020; Lackman, 2015). Some future scenarios show decreased vertical wind shear near the southeastern US coast which could foster more formation and intensification of tropical cyclones (Ting et al., 2019; Vecchi & Soden, 2007). Models have also been used to estimate the effects of specific environmental changes on hurricane strength. For example, Hurricane Matthew was simulated with end-of-century-projected sea-surface temperatures resulting in lower central pressure and consequent wind speed increases of 20 miles per hour (Jisan et al.,

2018). There is further evidence that increased sea-surface temperature has and will contribute to more rapid intensification of storms close to landfall (Emanuel, 2017).

Observations and models similarly provide a picture of increased precipitation associated with tropical cyclones (Stansfield et al., 2020). North Atlantic sea-surface temperature increases of 0.75-1.6°F since 1850 have led to increased extreme 3-hourly rainfall rates and 3-day total precipitation of 10% and 5%, respectively, for tropical cyclone strength storms with wind speeds reaching 42 mph, and even higher for hurricane strength (74mph) storms (Reed et al., 2022). Models that incorporate convection show significantly enhanced precipitation rates and totals for simulations of Hurricanes Katrina, Irma, Maria, and Florence (Patricola & Wehner, 2018; Reed et al., 2020).

Finally, it is important to consider the impacts of compounding factors. Future changes in wind and consequent storm surge, atmospheric moisture increase and precipitation intensity, forward speed of tropical cyclones, and sea level rise could amplify impacts (Gori et al., 2022).

## Marine climate impacts in South Carolina

### Key findings

- South Carolina's coast is low-lying and vulnerable to sea level rise. Sea levels have already risen by ~1 foot, will further rise by ~1 foot by 2050, and projections for sea level rise by 2150 range from 2 – 16 feet.
- Sea surface temperature increases off the Carolinas are statistically significant, and projected increases of 7 – 9 °F by 2100 would be among the highest nationally.
- *Ocean acidification* is currently stressing marine organisms and is projected to accelerate.
- Beyond sea level rise, South Carolina will experience compound changes (a combination of impacts that could be larger than each individually) in our coastal and marine waters including sea surface temperature, ocean acidification, salinity, *deoxygenation*, and potential disruptions to the Gulf Stream.
- Physical and chemical changes combine to create harmful impacts for marine ecosystems and coastal economies in South Carolina.

### Sea level rise

Increasing global temperature causes sea level rise. Globally, sea level rise has three main drivers — melting ice, warming ocean waters, and changes to water use on land. Melted ice adds water that was previously trapped in ice sheets and glaciers, water expands as it warms, and human uses of water either adds to (e.g., water previously

trapped in an underground aquifer is taken out and used) or removes (e.g., a dam that slows the flow of a river into the ocean) water flowing into the ocean. Regionally, sea level rise can also be affected by ocean circulation and changes in land elevation. Groundwater withdrawals can also cause land to sink, increasing impacts from sea level rise.

Measurements at tidal gauges provide direct evidence for sea level rise in South Carolina and around the world. For example, the tide gauge station in Charleston at the Cooper River has recorded data since September 13, 1899, showing a 1.1-foot rise during the past 100 years; the increase has accelerated since 2000 (NOAA, 2022c). In the past three decades satellites have supplemented gauge measurements with continuous monitoring of global sea level.

Emitting greenhouse gases causes global warming, which in turn changes the physical drivers affecting sea level rise. Based on current greenhouse gas concentrations, sea levels in South Carolina will rise an additional 10 – 14 inches by 2050 (Sweet et al., 2022). While the core mechanics of sea level rise are not debated, projections of it beyond 2050 vary because scientists continually improve understanding of complex interactions between multiple systems (ocean, land, and ice) and because of uncertainty associated with future emissions and the timing of certain physical processes, especially abrupt changes like when an ice sheet collapses. By 2150, we are almost certain to see approximately 2 feet of sea level rise, likely to see 3.5 – 7 feet if greenhouse gas emissions do not rapidly decrease, and may potentially see more than 16 feet (with further rising) if uncertain events like ice sheet collapses in Greenland or Antarctica occur (Figure 5.27; Sweet et al., 2022).

### Increasing frequency of coastal flood extremes

Sea level rise can combine with storm surges, tides, or heavy rainfall to produce compound-flood events (Figure 5.28; NOAA, 2022a, 2022c). Minor recurrent events cause disruptions and delays, while an additional 2 – 3 feet cause additional impacts, including damage to homes and businesses. These are sometimes referred to as extreme (sea level) events. In Charleston, extreme events are projected to occur 20 times as often by 2050 (Sweet et al., 2022).

### Ocean warming

The overwhelming majority (~90%) of the warming from greenhouse gases has been absorbed by the ocean, which has warmed by about 1.6°F this century (Fox-Kemper et al., 2021). The global oceans cover ~71% of the Earth's surface area, and water is a highly efficient absorber of heat compared to the atmosphere. Most of the increase in sea surface temperature has been in the past 50 years, and current rates of ocean heat-content increase are the highest in over 10,000 years (Fox-Kemper et al., 2021). Waters

off the southeastern US coast have warmed slightly faster than the global average due to proximity to the Gulf Stream, which draws from a warming tropical Atlantic (Fox-Kemper et al., 2021). Projections from the most recent generation of (CMIP6) climate models indicate a hotspot off the U.S. Atlantic coastline, with an increase of approximately 7-9°F by 2100 (Table 0.1; Intergovernmental Panel on Climate Change [IPCC], 2022; Ranasinghe et al., 2021). Coastal waters will warm faster than deep water, an effect of the gentle continental shelf slope and shallower water depths.

Warming ocean waters worsen other climate impacts, such as increasing the intensity of tropical hurricanes moving over them, as well as negatively affecting marine wildlife (Bindoff et al., 2019; Seneviratne et al., 2021). In addition to an increase in mean ocean temperature, temperatures can further spike within shorter periods; this is called a marine heatwave. If global warming exceeds 3.6°F (2°C), the southeast U.S. Atlantic coast is projected to be one of the worst areas impacted, experiencing marine heatwaves 20-times more often than present (Ranasinghe et al., 2021). The link between global warming and marine heatwaves is highly robust (Fox-Kemper et al., 2021). NOAA is already combining climate models with oceanographic station data to forecast marine heatwaves in our region up to 12 months in advance (Jacox et al., 2022).

### Ocean acidification

About a quarter (~20-30%) of $CO_2$ emissions enter the ocean; there is robust evidence that this uptake has caused ocean acidification (Canadell et al., 2021). At the regional level, ocean acidification is additionally affected by biological processes and run-off from land (Canadell et al., 2021). The surface ocean pH (a measure of acidity / alkalinity) has decreased at a rate of 0.017 to 0.027 units per decade since the late 1980s (indicating greater acidity), and estimates place the total pH decrease from human activities around 0.1 (Canadell et al., 2021; Tanhua et al., 2015). pH is a logarithmic scale, so a decline from 8.2 to 8.1 is a 26% increase in acidity. The rate of ocean acidification is predicted to accelerate in the SE region in the next 20-30 years, and projections of ocean acidification off the eastern coast of the U.S. under a high emissions scenario would approach pH levels not seen in the past 65 million years by the end of the century (Table 0.1; Canadell et al., 2021).

*Table 0.1 CMIP6 ensemble, Eastern North America Oceanic Region. Values in table are median projections, values in parenthetical are 5th and 95th percentiles, respectively. Future projections are in reference to baseline data from 1850 – 1900 (IPCC, 2022).*

| **Variable** | **RCP 4.5 (2081 – 2100)** | **RCP 8.5 (2081 – 2100)** |
|---|---|---|
| Sea Surface Temperature | + 4.7°F (2.7 \| 6.7) | + 7.6°F (4.7 \| 9.7) |
| pH at Surface | - 0.3 (-0.3 \| -0.2) | - 0.5 (-0.5 \| -0.4) |

### Increased salinity

The Atlantic has become saltier in the past 60 years, due to change in evaporation/precipitation balances over the ocean surface (Fox-Kemper et al., 2021). The link between anthropogenic $CO_2$ and salinity changes is robust (Eyring et al., 2021). Observed changes off the Carolinas coast are highly significant when analyzed alongside climate model projections (Friedman et al., 2017). Projections of salinity changes have improved in CMIP6, although there are increased biases when looking at only a small oceanic region (Fox-Kemper et al., 2021).

### Decreased dissolved oxygen

Ocean heating can reduce mixing and inhibit the process by which gasses dissolve in water. In the past 50 years, dissolved oxygen has decreased in the ocean's upper 1000 meters by 0.5 – 3.3% (Canadell et al., 2021). The link between anthropogenic $CO_2$ and changes in dissolved oxygen is highly robust (Canadell et al., 2021; Garcia-Soto et al., 2021). Deoxygenation serves as an ocean climate change indicator with implications for biological habitats; it is projected to accelerate globally (Canadell et al., 2021).

### Changing ocean currents

The Atlantic Meridional Overturning Circulation (a series of interconnected ocean currents, including the Gulf Stream off our coast) has slowed during the past 20 years and scientists are uncertain whether it could collapse under a high emissions scenario (Fox-Kemper et al., 2021). A combination of changes in water temperature and salinity, strongly affected by melting ice in Greenland, has affected the rate of deep water formation which drives this system of currents (Fox-Kemper et al., 2021). Climate models have underestimated observed rates of slowing, and scientists are actively researching the potential of a larger slowing or collapse (Fox-Kemper et al., 2021). Significant decreases in the Gulf Stream would further increase sea levels.

# Acronyms

CMIP5- Coupled Model Intercomparison Project Phase 5
CMIP6- Coupled Model Intercomparison Project Phase 6
CO2- Carbon Dioxide
GHCN-Daily- Global Historic Climatology Network
LOCA- Localized constructed analogs
NCEI- National Centers for Environmental Information
NOAA- National Oceanic and Atmospheric Administration
RCP- Representative Concentration Pathway

# References


Ahmadalipour, A., Moradkhani, H., & Svoboda, M. (2017). Centennial drought outlook over the CONUS using NASA-NEX downscaled climate ensemble. *International Journal of Climatology*, *37*(5), 2477–2491. https://doi.org/10.1002/joc.4859

Allen, J., & Lu, K. (2003). Modeling and Prediction of Future Urban Growth in the Charleston Region of South Carolina: a GIS-based Integrated Approach. *Conservation Ecology, 8*(2): 2. https://doi.org/10.5751/ES-00595-080202

Arias, P.A., N. Bellouin, E. Coppola, R.G. Jones, G. Krinner, J. Marotzke, V. Naik, M.D. Palmer, G.-K. Plattner, J. Rogelj, M. Rojas, J. Sillmann, T. Storelvmo, P.W. Thorne, B. Trewin, K. Achuta Rao, B. Adhikary, R.P. Allan, K. Armour, G. Bala, R. Barimalala,S. Berger, J.G. Canadell, C. Cassou, A. Cherchi, W. Collins, W.D. Collins, S.L. Connors, S. Corti, F. Cruz, F.J. Dentener, C. Dereczynski, A. Di Luca, A. Diongue Niang, F.J. Doblas-Reyes, A. Dosio, H. Douville, F. Engelbrecht, V. Eyring, E. Fischer, P. Forster, B. Fox-Kemper, J.S. Fuglestvedt, J.C. Fyfe, N.P. Gillett, L. Goldfarb, I. Gorodetskaya, J.M. Gutierrez, R. Hamdi, E. Hawkins, H.T. Hewitt, P. Hope, A.S. Islam, C. Jones, D.S. Kaufman, R.E. Kopp, Y. Kosaka, J. Kossin, S. Krakovska, J.-Y. Lee, J. Li,T. Mauritsen, T.K. Maycock, M. Meinshausen, S.-K. Min, P.M.S. Monteiro,T. Ngo-Duc, F. Otto, I. Pinto, A. Pirani, K. Raghavan, R. Ranasinghe, A.C. Ruane, L. Ruiz, J.-B. Sallée, B.H. Samset, S. Sathyendranath, S.I. Seneviratne, A.A. Sörensson, S. Szopa, I. Takayabu, A.-M. Tréguier, B. van den Hurk, R. Vautard, K. von Schuckmann, S. Zaehle, X. Zhang, and K. Zickfeld, 2021: Technical Summary. In *Climate Change 2021: The Physical Science Basis. Contribution of Working Group I to the Sixth Assessment Report of the Intergovernmental Panel on Climate Change* [Masson-Delmotte, V., P. Zhai, A. Pirani, S.L. Connors, C. Péan, S. Berger, N. Caud, Y. Chen, L. Goldfarb, M.I. Gomis, M. Huang, K. Leitzell, E. Lonnoy, J.B.R. Matthews, T.K. Maycock, T. Waterfield, O. Yelekçi, R. Yu, and B. Zhou (eds.)]. Cambridge University Press, Cambridge, UK and New York, NY,USA, pp. 33−144. doi:10.1017/9781009157896.002.B.

Barbero, R., Fowler, H. J., Blenkinsop, S., Westra, S., Moron, V., Lewis, E., Chan, S., Lenderink, G., Kendon, E., Guerreiro, S., Li, X.-F., Villalobos, R., Ali, H., & Mishra, V. (2019). A synthesis of hourly and daily precipitation extremes in different climatic regions. *Weather and Climate Extremes*, *26*, Article 100219. https://doi.org/10.1016/j.wace.2019.100219

Bindoff, N.L., W.W.L. Cheung, J.G. Kairo, J. Arístegui, V.A. Guinder, R. Hallberg, N. Hilmi, N. Jiao, M.S. Karim, L. Levin, S. O'Donoghue, S.R. Purca Cuicapusa, B. Rinkevich, T. Suga, A. Tagliabue, and P. Williamson, 2019: Changing Ocean, Marine Ecosystems, and Dependent Communities. In: *IPCC Special Report on the Ocean and Cryosphere in a Changing Climate* [H.-O. Pörtner, D.C. Roberts, V. Masson- Delmotte, P. Zhai, M. Tignor, E. Poloczanska, K. Mintenbeck, A. Alegría, M. Nicolai, A. Okem, J. Petzold, B. Rama, N.M. Weyer (eds.)]. Cambridge University Press, Cambridge, UK and New York, NY, USA, pp. 447–587. https://doi.org/10.1017/9781009157964.007

Blenkinsop, S., Fowler, H. J., Barbero, R., Chan, S. C., Guerreiro, S. B., Kendon, E., Lenderink, G., Lewis, E., Li, X.-F., Westra, S., Alexander, L., Allan, R. P., Berg, P., Dunn, R. J. H., Ekström, M., Evans, J. P., Holland, G., Jones, R., Kjellström, E., … Tye, M. R. (2018). The INTENSE project: Using observations and models to understand the past, present and future of sub-daily rainfall extremes. *Advances in Science and Research*, *15*, 117–126. https://doi.org/10.5194/asr-15-117-2018

Brown, V. M., Keim, B. D., & Black, A. W. (2019). Climatology and Trends in Hourly Precipitation for the Southeast United States. *Journal of Hydrometeorology*, *20*(8), 1737–1755. https://doi.org/10.1175/JHM-D-19-0004.1

Canadell, J.G., P.M.S. Monteiro, M.H. Costa, L. Cotrim da Cunha, P.M. Cox, A.V. Eliseev, S. Henson, M. Ishii, S. Jaccard, C. Koven, A. Lohila, P.K. Patra, S. Piao, J. Rogelj, S. Syampungani, S. Zaehle, and K. Zickfeld, 2021: Global Carbon and other Biogeochemical Cycles and Feedbacks. In *Climate Change 2021: The Physical Science Basis. Contribution of Working Group I to the Sixth Assessment Report of the Intergovernmental Panel on Climate Change* [Masson-Delmotte, V., P. Zhai, A. Pirani, S.L. Connors, C. Péan, S. Berger, N. Caud, Y. Chen, L. Goldfarb, M.I. Gomis, M. Huang, K. Leitzell, E. Lonnoy, J.B.R. Matthews, T.K. Maycock, T. Waterfield, O. Yelekçi, R. Yu, and B. Zhou (eds.)]. Cambridge University Press, Cambridge, United Kingdom and New York, NY, USA, pp. 673–816, doi:10.1017/9781009157896.007.

Curtis, S. (2008). The Atlantic multidecadal oscillation and extreme daily precipitation over the US and Mexico during the hurricane season. *Climate Dynamics*, *30*, 343–351. https://doi.org/10.1007/s00382-007-0295-0

Dahl, K., & Licker, R. (2021). *Too Hot to Work: Assessing the Threats Climate Change Poses to Outdoor Workers.* Union of Concerned Scientists. https://www.ucsusa.org/resources/too-hot-to-work

Diem, J. E. (2006). Synoptic-Scale Controls of Summer Precipitation in the Southeastern United States. *Journal of Climate*, *19*(4), 613–621. https://doi.org/10.1175/JCLI3645.1

Easterling, D.R., K.E. Kunkel, J.R. Arnold, T. Knutson, A.N. LeGrande, L.R. Leung, R.S. Vose, D.E. Waliser, and M.F. Wehner, 2017: Precipitation change in the United States. In: *Climate Science Special Report*: Fourth National Climate Assessment, Volume I [Wuebbles, D.J., D.W. Fahey, K.A. Hibbard, D.J. Dokken, B.C. Stewart, and T.K. Maycock (eds.)]. U.S. Global Change Research Program, Washington, DC, USA, pp. 207-230, doi: 10.7930/J0H993CC.

Emanuel, K. (2017). Will Global Warming Make Hurricane Forecasting More Difficult? *Bulletin of the American Meteorological Society*, *98*(3), 495–501. https://doi.org/10.1175/BAMS-D-16-0134.1

Emanuel, K. (2021). Response of Global Tropical Cyclone Activity to Increasing CO2: Results from Downscaling CMIP6 Models. *Journal of Climate*, *34*(1), 57–70. https://doi.org/10.1175/JCLI-D-20-0367.1

Engström, J., & Keellings, D. (2018). Drought in the Southeastern USA: An assessment of downscaled CMIP5 models. *Climate Research*, *74*(3), 251–262. https://doi.org/10.3354/cr01502

Eyring, V., N.P. Gillett, K.M. Achuta Rao, R. Barimalala, M. Barreiro Parrillo, N. Bellouin, C. Cassou, P.J. Durack, Y. Kosaka, S. McGregor, S. Min, O. Morgenstern, and Y. Sun, 2021: Human Influence on the Climate System. In *Climate Change 2021: The Physical Science Basis. Contribution of Working Group I to the Sixth Assessment Report of the Intergovernmental Panel on Climate Change* [Masson-Delmotte, V., P. Zhai, A. Pirani, S.L. Connors, C. Péan, S. Berger, N. Caud, Y. Chen, L. Goldfarb, M.I. Gomis, M. Huang, K. Leitzell, E. Lonnoy, J.B.R. Matthews, T.K. Maycock, T. Waterfield, O. Yelekçi, R. Yu, and B. Zhou (eds.)]. Cambridge University Press, Cambridge, United Kingdom and New York, NY, USA, pp. 423–552.

Fischer, E. M., & Knutti, R. (2016). Observed heavy precipitation increase confirms theory and early models. *Nature Climate Change*, *6*, 986–991. https://doi.org/10.1038/nclimate3110

Forestieri, A., Arnone, E., Blenkinsop, S., Candela, A., Fowler, H., & Noto, L. V. (2018). The impact of climate change on extreme precipitation in Sicily, Italy. *Hydrological Processes*, *32*(3), 332–348. https://doi.org/10.1002/hyp.11421

Fox-Kemper, B., H.T. Hewitt, C. Xiao, G. Aðalgeirsdóttir, S.S. Drijfhout, T.L. Edwards, N.R. Golledge, M. Hemer, R.E. Kopp, G. Krinner, A. Mix, D. Notz, S. Nowicki, I.S. Nurhati, L. Ruiz, J.-B. Sallée, A.B.A. Slangen, and Y. Yu, 2021: Ocean, Cryosphere and Sea Level Change. In *Climate Change 2021: The Physical Science Basis. Contribution of Working Group I to the Sixth Assessment Report of the Intergovernmental Panel on Climate Change* [Masson-Delmotte, V., P. Zhai, A. Pirani, S.L. Connors, C. Péan, S. Berger, N. Caud, Y. Chen, L. Goldfarb, M.I. Gomis, M. Huang, K. Leitzell, E. Lonnoy, J.B.R. Matthews, T.K. Maycock, T. Waterfield, O. Yelekçi, R. Yu, and B. Zhou (eds.)]. Cambridge University Press, Cambridge, United Kingdom and New York, NY, USA, pp. 1211–1362, doi:10.1017/9781009157896.011.

Friedman, A. R., Reverdin, G., Khodri, M., & Gastineau, G. (2017). A new record of Atlantic sea surface salinity from 1896 to 2013 reveals the signatures of climate variability and long-term trends. *Geophysical Research Letters*, *44*(4), 1866–1876. https://doi.org/10.1002/2017GL072582

Garcia-Soto, C., Cheng, L., Caesar, L., Schmidtko, S., Jewett, E. B., Cheripka, A., Rigor, I., Caballero, A., Chiba, S., Báez, J. C., Zielinski, T., & Abraham, J. P. (2021). An Overview of Ocean Climate Change Indicators: Sea Surface Temperature, Ocean Heat Content, Ocean pH, Dissolved Oxygen Concentration, Arctic Sea Ice Extent, Thickness and Volume, Sea Level and Strength of the AMOC (Atlantic Meridional Overturning Circulation). *Frontiers in Marine Science*, *8*. https://www.frontiersin.org/article/10.3389/fmars.2021.642372

Gori, A., Lin, N., Xi, D., & Emanuel, K. (2022). Tropical cyclone climatology change greatly exacerbates US extreme rainfall–surge hazard. *Nature Climate Change*, *12*, 171–178. https://doi.org/10.1038/s41558-021-01272-7

Grabowski, W. W., & Prein, A. F. (2019). Separating Dynamic and Thermodynamic Impacts of Climate Change on Daytime Convective Development over Land. *Journal of Climate*, *32*(16), 5213–5234. https://doi.org/10.1175/JCLI-D-19-0007.1

Hayhoe, K., J. Edmonds, R.E. Kopp, A.N. LeGrande, B.M. Sanderson, M.F. Wehner, and D.J. Wuebbles, 2017: Climate models, scenarios, and projections. In: *Climate Science Special Report: Fourth National Climate Assessment, Volume I* [Wuebbles, D.J., D.W. Fahey, K.A. Hibbard, D.J. Dokken, B.C. Stewart, and T.K. Maycock (eds.)]. U.S. Global Change Research Program, Washington, DC, USA, pp. 133-160, doi: 10.7930/J0WH2N54.

Huang, H., Winter, J. M., Osterberg, E. C., Horton, R. M., & Beckage, B. (2017). Total and Extreme Precipitation Changes over the Northeastern United States. *Journal of Hydrometeorology*, *18*(6), 1783–1798. https://doi.org/10.1175/JHM-D-16-0195.1

Intergovernmental Panel on Climate Change. (2022). *Regional information (Advanced)*. IPCC WGI Interactive Atlas. https://interactive-atlas.ipcc.ch/

Intergovernmental Panel on Climate Change, 2021: Summary for Policymakers. In: *Climate Change 2021: The Physical Science Basis. Contribution of Working Group I to the Sixth Assessment Report of the Intergovernmental Panel on Climate Change* [Masson-Delmotte, V., P. Zhai, A. Pirani, S.L. Connors, C. Péan, S. Berger, N. Caud, Y. Chen, L. Goldfarb, M.I. Gomis, M. Huang, K. Leitzell, E. Lonnoy, J.B.R. Matthews, T.K. Maycock, T. Waterfield, O. Yelekçi, R. Yu, and B. Zhou (eds.)]. Cambridge University Press, Cambridge, United Kingdom and New York, NY, USA, pp. 3–32, doi:10.1017/9781009157896.001

Jacox, M. G., Alexander, M. A., Amaya, D., Becker, E., Bograd, S. J., Brodie, S., Hazen, E. L., Pozo Buil, M., & Tommasi, D. (2022). Global seasonal forecasts of marine heatwaves. *Nature*, *604*, Article 7906. https://doi.org/10.1038/s41586-022-04573-9

Jalowska, A. M., Spero, T. L., & Bowden, J. H. (2021). Projecting changes in extreme rainfall from three tropical cyclones using the design-rainfall approach. *Npj Climate and Atmospheric Science*, *4*, Article 23. https://doi.org/10.1038/s41612-021-00176-9

Jing, R., & Lin, N. (2020). An Environment-Dependent Probabilistic Tropical Cyclone Model. *Journal of Advances in Modeling Earth Systems*, *12*(3), 18. https://doi.org/10.1029/2019MS001975

Jing, R., Lin, N., Emanuel, K., Vecchi, G., & Knutson, T. R. (2021). A Comparison of Tropical Cyclone Projections in a High-Resolution Global Climate Model and from Downscaling by Statistical and Statistical-Deterministic Methods. *Journal of Climate*, *34*(23), 9349–9364. https://doi.org/10.1175/JCLI-D-21-0071.1

Jisan, M. A., Bao, S., Pietrafesa, L. J., Shen, D., Gayes, P. T., & Hallstrom, J. (2018). Hurricane Matthew (2016) and its impact under global warming scenarios. *Modeling Earth Systems and Environment*, *4*(1), 97–109. https://doi.org/10.1007/s40808-018-0420-6

Keellings, D. (2016). Evaluation of downscaled CMIP5 model skill in simulating daily maximum temperature over the southeastern United States. *International Journal of Climatology*, *36*(12), 4172–4180. https://doi.org/10.1002/joc.4612

Keellings, D., & Engström, J. (2019). The Future of Drought in the Southeastern U.S.: Projections from Downscaled CMIP5 Models. *Water*, *11*(2), 259. https://doi.org/10.3390/w11020259

Knutson, T., Camargo, S. J., Chan, J. C. L., Emanuel, K., Ho, C.-H., Kossin, J., Mohapatra, M., Satoh, M., Sugi, M., Walsh, K., & Wu, L. (2020). Tropical Cyclones and Climate Change Assessment: Part II: Projected Response to Anthropogenic Warming. *Bulletin of the American Meteorological Society*, *101*(3), Article E303-E322. https://doi.org/10.1175/BAMS-D-18-0194.1

Kossin, J. P., Knapp, K. R., Olander, T. L., & Velden, C. S. (2020). Global increase in major tropical cyclone exceedance probability over the past four decades. *Proceedings of the National Academy of Sciences*, *117*(22), 11975–11980. https://doi.org/10.1073/pnas.1920849117

Kunkel, K.E., D.R. Easterling, A. Ballinger, S. Bililign, S.M. Champion, D.R. Corbett, K.D. Dello, J. Dissen, G.M. Lackmann, R.A. Luettich, Jr., L.B. Perry, W.A. Robinson, L.E. Stevens, B.C. Stewart, and A.J. Terando, 2020a: *North Carolina Climate Science Report*. North Carolina Institute for Climate Studies, 233 pp. https://ncics.org/nccsr

Kunkel, K. E., Karl, T. R., Squires, M. F., Yin, X., Stegall, S. T., & Easterling, D. R. (2020b). Precipitation Extremes: Trends and Relationships with Average Precipitation and Precipitable Water in the Contiguous United States. *Journal of Applied Meteorology and Climatology*, *59*(1), 125–142. https://doi.org/10.1175/JAMC-D-19-0185.1

Kunkel, K. E., Stevens, S. E., Stevens, L. E., & Karl, T. R. (2020c). Observed Climatological Relationships of Extreme Daily Precipitation Events With Precipitable Water and Vertical Velocity in the Contiguous United States. *Geophysical Research Letters*, *47*(12), Article e2019GL086721. https://doi.org/10.1029/2019GL086721

Kunkel, K.E., R. Frankson, J. Runkle, S.M. Champion, L.E. Stevens, D.R. Easterling, B.C. Stewart, A. McCarrick, and C.R. Lemery (Eds.), 2022: State Climate Summaries for the United States 2022. NOAA Technical Report NESDIS 150. NOAA/NESDIS, Silver Spring, MD.

Labosier, C. F., & Quiring, S. M. (2013). Hydroclimatology of the Southeastern USA. *Climate Research*, *57*, 157–171. https://doi.org/10.3354/cr01166

Lackmann, G. M. (2015). Hurricane Sandy before 1900 and after 2100. *Bulletin of the American Meteorological Society*, *96*(4), 547–560. https://doi.org/10.1175/BAMS-D-14-00123.1

Lehmann, J., Coumou, D., & Frieler, K. (2015). Increased record-breaking precipitation events under global warming. *Climatic Change*, *132*, 501–515. https://doi.org/10.1007/s10584-015-1434-y

Loeb, N. G., Johnson, G. C., Thorsen, T. J., Lyman, J. M., Rose, F. G., & Kato, S. (2021). Satellite and Ocean Data Reveal Marked Increase in Earth's Heating Rate. *Geophysical Research Letters*, *48*(13), Article e2021GL093047. https://doi.org/10.1029/2021GL093047

Mallard, M. S., Lackmann, G. M., & Aiyyer, A. (2013). Atlantic Hurricanes and Climate Change. Part II: Role of Thermodynamic Changes in Decreased Hurricane Frequency. *Journal of Climate*, *26*(21), 8513–8528. https://doi.org/10.1175/JCLI-D-12-00183.1

Menne, M. J., Durre, I., Vose, R. S., Gleason, B. E., & Houston, T. G. (2012). An Overview of

the Global Historical Climatology Network-Daily Database. *Journal of Atmospheric and Oceanic Technology*, *29*(7), 897–910. https://doi.org/10.1175/JTECH-D-11-00103.1

Moraglia, G., Brattich, E., & Carbone, G.J. (2022, Forthcoming). Precipitation trends in North and South Carolina, USA. *Journal of Hydrology: regional studies*.

Moss, R. H., Edmonds, J. A., Hibbard, K. A., Manning, M. R., Rose, S. K., van Vuuren, D. P., Carter, T. R., Emori, S., Kainuma, M., Kram, T., Meehl, G. A., Mitchell, J. F. B., Nakicenovic, N., Riahi, K., Smith, S. J., Stouffer, R. J., Thomson, A. M., Weyant, J. P., & Wilbanks, T. J. (2010). The next generation of scenarios for climate change research and assessment. *Nature*, *463*, 747–756. https://doi.org/10.1038/nature08823

National Oceanic and Atmospheric Administration. (2022a). *Station ID: 8665530*. NOAA Tides & Currents Data API. https://api.tidesandcurrents.noaa.gov/dpapi/prod/webapi/htf/htf_annual.json?station=8665530&units=english

2National Oceanic and Atmospheric Administration. (2022b). *Trends in Atmospheric Carbon Dioxide.* Global Monitoring Laboratory. https://gml.noaa.gov/ccgg/trends/

National Oceanic and Atmospheric Administration. (2022c, May 25). *Charleston, Cooper River Entrance, SC - Station ID: 8665530*. Tides & Currents. https://tidesandcurrents.noaa.gov/stationhome.html?id=8665530#info

O'Gorman, P., & Schneider, T. (2009). The physical basis for increases in precipitation extremes in simulations of 21st-century climate change. *Proceedings of the National Academy of Sciences*, *106*(35), 14773–14777. https://doi.org/10.1073/pnas.0907610106

Paerl, H. W., Hall, N. S., Hounshell, A. G., Luettich, R. A., Rossignol, K. L., Osburn, C. L., & Bales, J. (2019). Recent increase in catastrophic tropical cyclone flooding in coastal North Carolina, USA: Long-term observations suggest a regime shift. *Scientific Reports*, *9*, Article 10620. https://doi.org/10.1038/s41598-019-46928-9

Patricola, C. M., & Wehner, M. F. (2018). Anthropogenic influences on major tropical cyclone events. *Nature*, *563*, Article 7731. https://doi.org/10.1038/s41586-018-0673-2

Pierce, D. W., Cayan, D. R., & Thrasher, B. L. (2014). Statistical Downscaling Using Localized Constructed Analogs (LOCA). *Journal of Hydrometeorology*, *15*(6), 2558–2585. https://doi.org/10.1175/JHM-D-14-0082.1

Powell, E. J., & Keim, B. D. (2015). Trends in Daily Temperature and Precipitation Extremes for the Southeastern United States: 1948–2012. *Journal of Climate*, *28*(4), 1592–1612. https://doi.org/10.1175/JCLI-D-14-00410.1

Prein, A. F., Rasmussen, R. M., Ikeda, K., Liu, C., Clark, M. P., & Holland, G. J. (2017). The future intensification of hourly precipitation extremes. *Nature Climate Change*, *7*, 48–52. https://doi.org/10.1038/nclimate3168

Qian, J.-H., Viner, B., Noble, S., & Werth, D. (2021). Precipitation Characteristics of Warm Season Weather Types in the Southeastern United States of America. *Atmosphere*, *12*(8), Article 1001. https://doi.org/10.3390/atmos12081001

Ranasinghe, R., A.C. Ruane, R. Vautard, N. Arnell, E. Coppola, F.A. Cruz, S. Dessai, A.S. Islam, M. Rahimi, D. Ruiz Carrascal, J. Sillmann, M.B. Sylla, C. Tebaldi, W. Wang,

and R. Zaaboul, 2021: Climate Change Information for Regional Impact and for Risk Assessment. In *Climate Change 2021: The Physical Science Basis. Contribution of Working Group I to the Sixth Assessment Report of the Intergovernmental Panel on Climate Change* [Masson- Delmotte, V., P. Zhai, A. Pirani, S.L. Connors, C. Péan, S. Berger, N. Caud, Y. Chen, L. Goldfarb, M.I. Gomis, M. Huang, K. Leitzell, E. Lonnoy, J.B.R. Matthews, T.K. Maycock, T. Waterfield, O. Yelekçi, R. Yu, and B. Zhou (eds.)]. Cambridge University Press, Cambridge, United Kingdom and New York, NY, USA, pp. 1767–1926, doi:10.1017/9781009157896.014.

Reed, K. A., Stansfield, A. M., Wehner, M. F., & Zarzycki, C. M. (2020). Forecasted attribution of the human influence on Hurricane Florence. *Science Advances*, *6*(1), Article eaaw9253. https://doi.org/10.1126/sciadv.aaw9253

Reed, K. A., Wehner, M. F., & Zarzycki, C. M. (2022). Attribution of 2020 hurricane season extreme rainfall to human-induced climate change. *Nature Communications*, *13*, Article 1905. https://doi.org/10.1038/s41467-022-29379-1

Rickenbach, T. M., Nieto-Ferreira, R., Zarzar, C., & Nelson, B. (2015). A seasonal and diurnal climatology of precipitation organization in the southeastern United States. *Quarterly Journal of the Royal Meteorological Society*, *141*(690), 1938–1956. https://doi.org/10.1002/qj.2500

Risser, M. D., & Wehner, M. F. (2017). Attributable Human-Induced Changes in the Likelihood and Magnitude of the Observed Extreme Precipitation during Hurricane Harvey. *Geophysical Research Letters*, *44*(24), 12,457-12,464. https://doi.org/10.1002/2017GL075888

Rupp, D. E. (2016). An evaluation of 20th century climate for the Southeastern United States as simulated by Coupled Model Intercomparison Project Phase 5 (CMIP5) global climate models. In *An evaluation of 20th century climate for the Southeastern United States as simulated by Coupled Model Intercomparison Project Phase 5 (CMIP5) global climate models* (USGS Numbered Series No. 2016–1047; Open-File Report, Vols. 2016–1047, p. 32). U.S. Geological Survey. https://doi.org/10.3133/ofr20161047

Seneviratne, S.I., X. Zhang, M. Adnan, W. Badi, C. Dereczynski, A. Di Luca, S. Ghosh, I. Iskandar, J. Kossin, S. Lewis, F. Otto, I. Pinto, M. Satoh, S.M. Vicente-Serrano, M. Wehner, and B. Zhou, 2021: Weather and Climate Extreme Events in a Changing Climate. In *Climate Change 2021: The Physical Science Basis. Contribution of Working Group I to the Sixth Assessment Report of the Intergovernmental Panel on Climate Change* [Masson- Delmotte, V., P. Zhai, A. Pirani, S.L. Connors, C. Péan, S. Berger, N. Caud, Y. Chen, L. Goldfarb, M.I. Gomis, M. Huang, K. Leitzell, E. Lonnoy, J.B.R. Matthews, T.K. Maycock, T. Waterfield, O. Yelekçi, R. Yu, and B. Zhou (eds.)]. Cambridge University Press, Cambridge, United Kingdom and New York, NY, USA, pp. 1513–1766, doi:10.1017/9781009157896.013.

Smith, C. J., Kramer, R. J., Myhre, G., Alterskjær, K., Collins, W., Sima, A., Boucher, O., Dufresne, J.-L., Nabat, P., Michou, M., Yukimoto, S., Cole, J., Paynter, D., Shiogama, H., O'Connor, F. M., Robertson, E., Wiltshire, A., Andrews, T., Hannay, C., … Forster, P. M. (2020). Effective radiative forcing and adjustments in CMIP6 models. *Atmospheric Chemistry and Physics*, *20*(16), 9591–9618. https://doi.org/10.5194/acp-20-

9591-2020
Sobel, A. H., Wing, A. A., Camargo, S. J., Patricola, C. M., Vecchi, G. A., Lee, C.-Y., & Tippett, M. K. (2021). Tropical Cyclone Frequency. *Earth's Future*, *9*(12), 24. https://doi.org/10.1029/2021EF002275
Soulé, P. T. (2022). Temporal Patterns of Drought Frequency and Severity in North Carolina, 1920–2019 and the Drought Gap of the 1960s–1970s. *Southeastern Geographer*, *62*(1), 25–37. https://doi.org/10.1353/sgo.2022.0003
Stansfield, A. M., Reed, K. A., & Zarzycki, C. M. (2020). Changes in Precipitation From North Atlantic Tropical Cyclones Under RCP Scenarios in the Variable-Resolution Community Atmosphere Model. *Geophysical Research Letters*, *47*(12), 10. https://doi.org/10.1029/2019GL086930
Sweet, W.V., B.D. Hamlington, R.E. Kopp, C.P. Weaver, P.L. Barnard, D. Bekaert, W. Brooks, M. Craghan, G. Dusek, T. Frederikse, G. Garner, A.S. Genz, J.P. Krasting, E. Larour, D. Marcy, J.J. Marra, J. Obeysekera, M. Osler, M. Pendleton, D. Roman, L. Schmied, W. Veatch, K.D. White, and C. Zuzak, 2022: Global and Regional Sea Level Rise Scenarios for the United States: Up-dated Mean Projections and Extreme Water Level Probabilities Along U.S. Coastlines. NOAA Technical Report NOS 01. National Oceanic and Atmospheric Administration, National Ocean Service, Silver Spring, MD, 111 pp. https://oceanservice.noaa.gov/hazards/sealevelrise/noaa-nos-techrpt01-global-regional-SLR-scenarios-US.pdf.
Tabari, H. (2020). Climate change impact on flood and extreme precipitation increases with water availability. *Scientific Reports*, *10*, Article 13768. https://doi.org/10.1038/s41598-020-70816-2
Tanhua, T., Orr, J. C., Lorenzoni, L., & Hansson, L. (2015). Monitoring Ocean Carbon and Ocean Acidification. *World Meteorological Organization Bulletin*, *64*(1), 48–51.
Taylor, K. E., Stouffer, R. J., & Meehl, G. A. (2012). An Overview of CMIP5 and the Experiment Design. *Bulletin of the American Meteorological Society*, *93*(4), 485–498. https://doi.org/10.1175/BAMS-D-11-00094.1
Terando, A. J., Costanza, J., Belyea, C., Dunn, R. R., McKerrow, A., & Collazo, J. A. (2014). The Southern Megalopolis: Using the Past to Predict the Future of Urban Sprawl in the Southeast U.S. *PLOS ONE*, *9*(7), Article e102261. https://doi.org/10.1371/journal.pone.0102261
Ting, M., Kossin, J. P., Camargo, S. J., & Li, C. (2019). Past and Future Hurricane Intensity Change along the U.S. East Coast. *Scientific Reports*, *9*, Article 7795. https://doi.org/10.1038/s41598-019-44252-w
Trenberth, K. E., Dai, A., Rasmussen, R. M., & Parsons, D. B. (2003). The Changing Character of Precipitation. *Bulletin of the American Meteorological Society*, *84*(9), 1205–1218. https://doi.org/10.1175/BAMS-84-9-1205
van der Wiel, K., Kapnick, S. B., van Oldenborgh, G. J., Whan, K., Philip, S., Vecchi, G. A., Singh, R. K., Arrighi, J., & Cullen, H. (2017). Rapid attribution of the August 2016 flood-inducing extreme precipitation in south Louisiana to climate change. *Hydrology and Earth System Sciences*, *21*(2), 897–921. https://doi.org/10.5194/hess-21-

897-2017

van Oldenborgh, G. J., van der Wiel, K., Sebastian, A., Singh, R., Arrighi, J., Otto, F., Haustein, K., Li, S., Vecchi, G., & Cullen, H. (2017). Attribution of extreme rainfall from Hurricane Harvey, August 2017. *Environmental Research Letters*, *12*(12), Article 124009. https://doi.org/10.1088/1748-9326/aa9ef2

Vecchi, G. A., & Soden, B. J. (2007). Global Warming and the Weakening of the Tropical Circulation. *Journal of Climate*, *20*(17), 4316–4340. https://doi.org/10.1175/JCLI4258.1

Vose, R. S., Applequist, S., Squires, M., Durre, I., Menne, M. J., Williams, C. N., Fenimore, C., Gleason, K., & Arndt, D. (2014). Improved Historical Temperature and Precipitation Time Series for U.S. Climate Divisions. *Journal of Applied Meteorology and Climatology*, *53*(5), 1232–1251. https://doi.org/10.1175/JAMC-D-13-0248.1

Wu, L., Zhao, H., Wang, C., Cao, J., & Liang, J. (2022). Understanding of the Effect of Climate Change on Tropical Cyclone Intensity: A Review. *Advances in Atmospheric Sciences*, *39*(2), 205–221. https://doi.org/10.1007/s00376-021-1026-x

# Figures

Figure 5.1 Earth's radiation budget ..... 2
Figure 5.2: Climate model simulated temperature with and without anthropogenic forcing plotted against observed temperature (Source: IPCC, 2021). ..... 3
Figure 5.3: South Carolina average annual temperature. ..... 4
Figure 5.4: Global, Contiguous United States, and South Carolina average temperature anomalies from 20th century mean. ..... 5
Figure 5.5: Spring maximum temperature trend, 1900-2020. ..... 6
Figure 5.6: Summer maximum temperature trend, 1900-2020 ..... 7
Figure 5.7: : Winter maximum temperature trend, 1900-2020 ..... 8
Figure 5.8: Summer minimum temperature trend, 1900-2020 ..... 9
Figure 5.9: 1900-2020 Little Mountain, South Carolina Spring maximum temperature anomalies (from 1900-1960 average) ..... 10
Figure 5.10: Modeled vs. observed annual, state-averaged maximum and minimum temperature ..... 11
Figure 5.11: Model simulated average temperature for South Carolina. Projections are measured as departures (anomalies) from the 1991-2020 mean (RCP 4.5 emissions scenario). ..... 12
Figure 5.12: Same as Figure 5.11, but for the high emissions scenario (RCP 8.5). ..... 13
Figure 5.13: Projected increase in the number of days per year with maximum temperature above 95°F (RCP 4.5 emissions scenario). ..... 14
Figure 5.14: Projected increase in the number of days per year with maximum temperature above 95°F (RCP 8.5 emissions scenario) ..... 15
Figure 5.15: Projected number of days per year with maximum temperature above 75°F (RCP 8.5 emissions scenario). ..... 16
Figure 5.16: Projected number of days per year with minimum temperature below 32°F (RCP 8.5 emissions scenario). ..... 17
Figure 5.17: State-averaged total annual precipitation. ..... 18
Figure 5.18: Summer precipitation trend, 1900-2020. ..... 19
Figure 5.19: Santuck, SC summer precipitation anomalies from 1901-1960 mean. ..... 20
Figure 5.20: Model projected annual precipitation as percentage greater or less than 1991-2020 mean. ..... 21
Figure 5.21: Average recurrence interval of 1-day precipitation depths calculated for separate 50-year periods. Shading is lightest for earliest period (1910-1959) and darkest for most recent period (1970-2019). ..... 22
Figure 5.22: Average recurrence interval of 1-day precipitation depths calculated separately for 1910-2000, and for 1910-2020. ..... 23
Figure 5.23: Areas experiencing 100-, 200-, 500-, and 1000-year rainfall events due to one or more of the recent extreme storms. (Data provided by SC Department of Natural Resources.).. 24
Figure 5.24: Palmer Hydrological Drought Index 1895-2020. ..... 25
Figure 5.25: Variability of Drought across South Carolina (Fall 2016) ..... 26
Figure 5.26: Tropical Cyclones affecting South Carolina, 1851-2020. ..... 27
Figure 5.27: Charleston sea level change projections (Adapted from Sweet et al., 2022). ..... 28
Figure 5.28: Annual Flood Count and Sea Level at Charleston Gauge. Sea level is relative to the current National Tidal Datum Epoch, 1983-2001 ..... 29

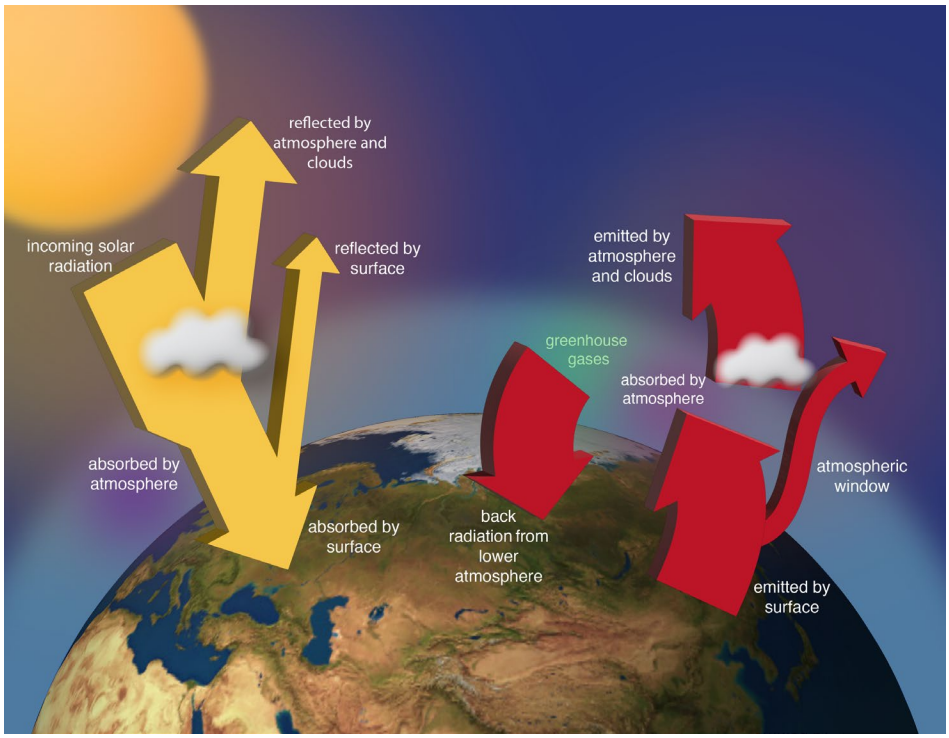


*Figure 5.1 Earth's radiation budget*

ALT / Screenreader text: This figure shows representing Earth's radiation budget. Arrows on the left side of the diagram show incoming solar radiation, some of which is reflected by the atmosphere/clouds/Earth's surface, some of which is absorbed by the atmosphere, and some of which is absorbed by Earth's surface. Most is absorbed by the Earth's surface. Arrows on the right side show outgoing radiation emitted by the Earth's surface – a large portion of which is absorbed by the atmosphere and clouds – and radiation emitted by the atmosphere – some back down to Earth's surface, some to space.

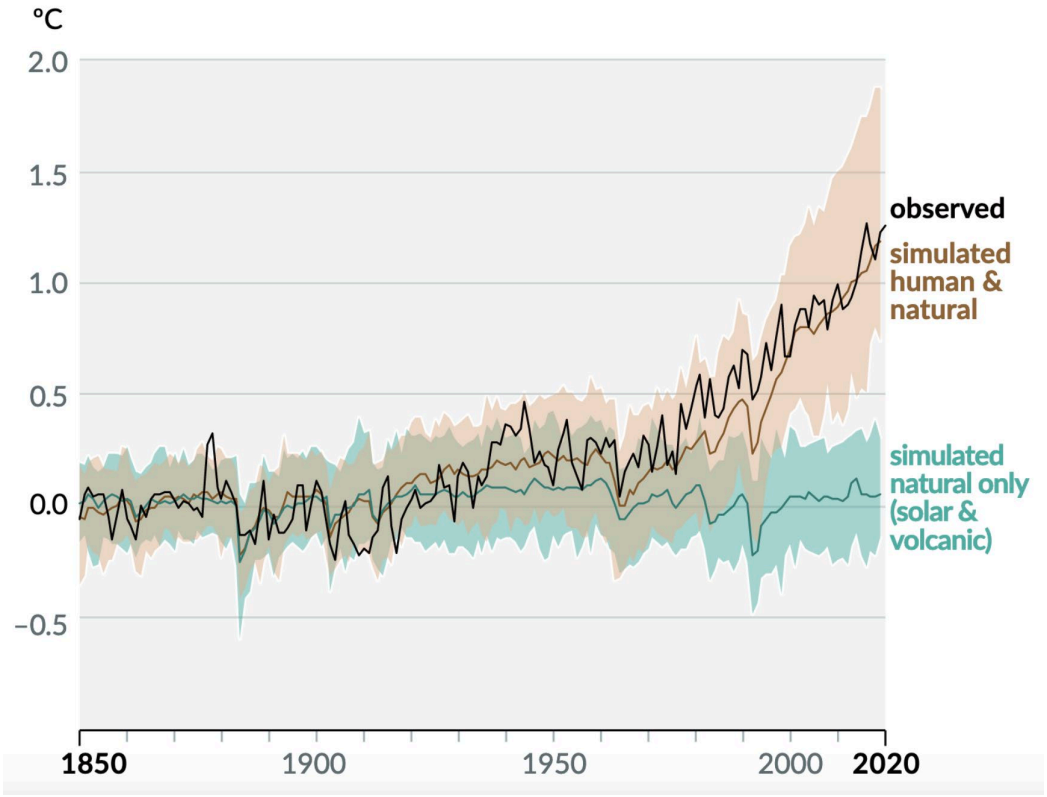


*Figure 5.2: Climate model simulated temperature with and without anthropogenic forcing plotted against observed temperature (Source: IPCC, 2021).*

ALT / Screenreader text: The figure shows three lines on an x-axis of years (ranging from 1850 to 2020) and a y-axis of degrees Celsius (ranging from –0.5 to 2.0). The first line shows observed global temperature anomalies from 1850-2020. It shows interannual variability and two marked increases: about 0.5°C from 1905-1945, and about 1.25°C from 1960-2020. The second line shows temperature simulated by a climate model using natural forcing only ; it stays near zero through all years, except for a few negative spikes associated with major volcanic eruptions. The third line shows temperature simulated by a climate model using both natural and anthropogenic (i.e., greenhouse gas) forcing. It closely matches the observed global temperature pattern.

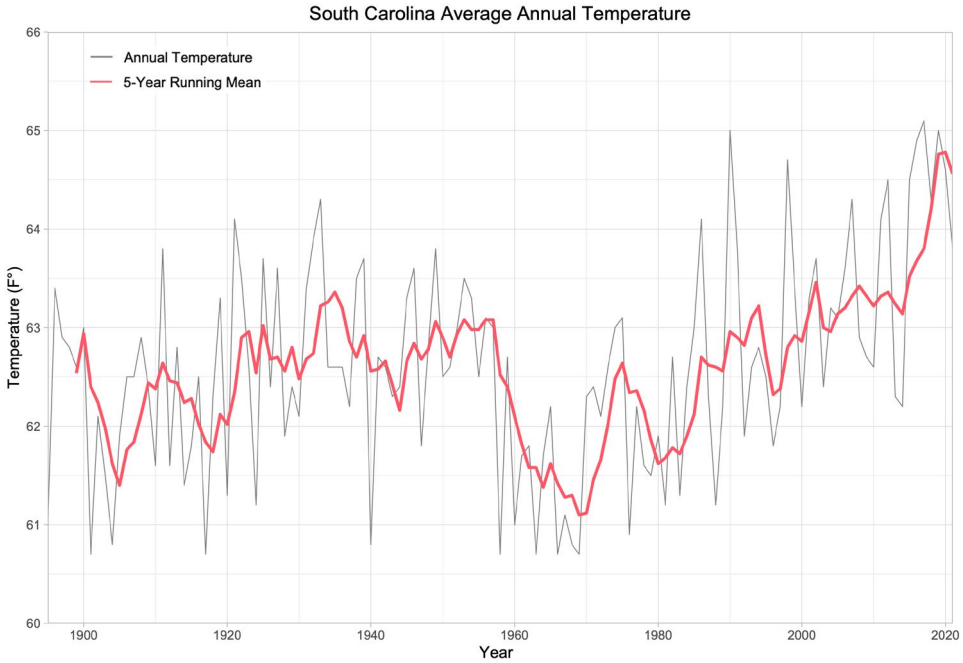


*Figure 5.3: South Carolina average annual temperature.*

ALT / Screenreader text: This figure shows South Carolina's average annual temperature as two lines on an x-axis that ranges from 1900 – 2020, and a y-axis ranging from 60 to 66 degrees. The first line shows annual temperature, the second line shows a smoothed 5-year running mean. The running mean averages between 61.5 and 63 degrees Fahrenheit from 1900 to 1960, dips down to 61 – 62 from 1960 to 1980, and increases from 1980 to 2020, reaching close to 65 by 2020.

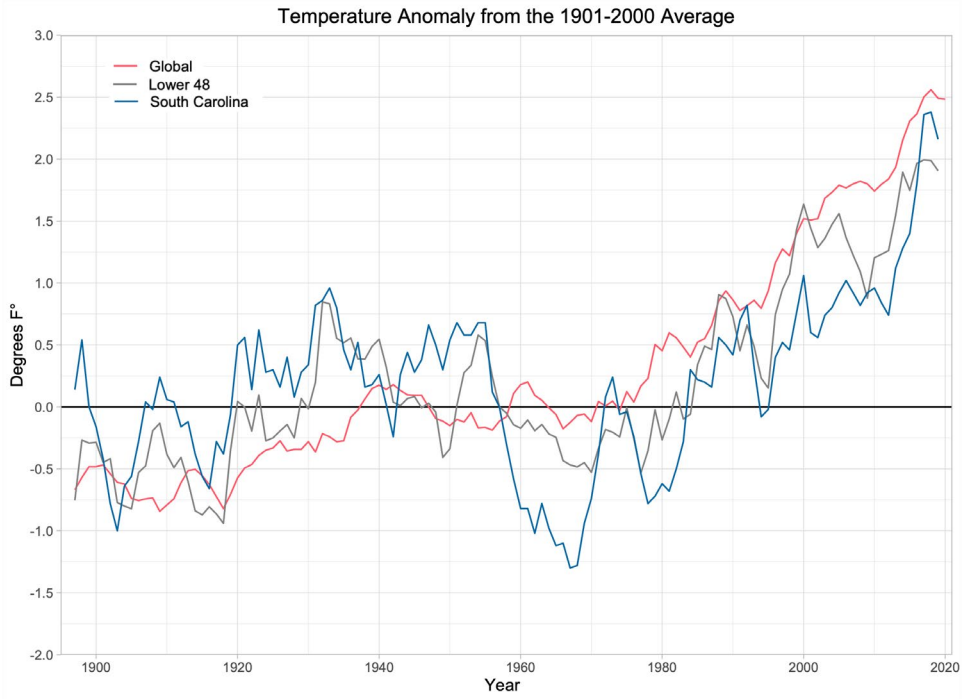


*Figure 5.4: Global, Contiguous United States, and South Carolina average temperature anomalies from 20th century mean.*

ALT / Screenreader text: This figure is a line graph comparing changes in South Carolina, the contiguous United States, and global average temperature since 1900. The x-axis shows years 1900 to 2020. Temperature, expressed as anomalies from the 20th century mean is shown on the y-axis and ranges from –2 to 3 degrees Fahrenheit. All three lines show variability, with South Carolina's having the most. All three lines increase over time, especially since 1970, reaching a 2-to-2.5-degree Fahrenheit anomaly by 2020.

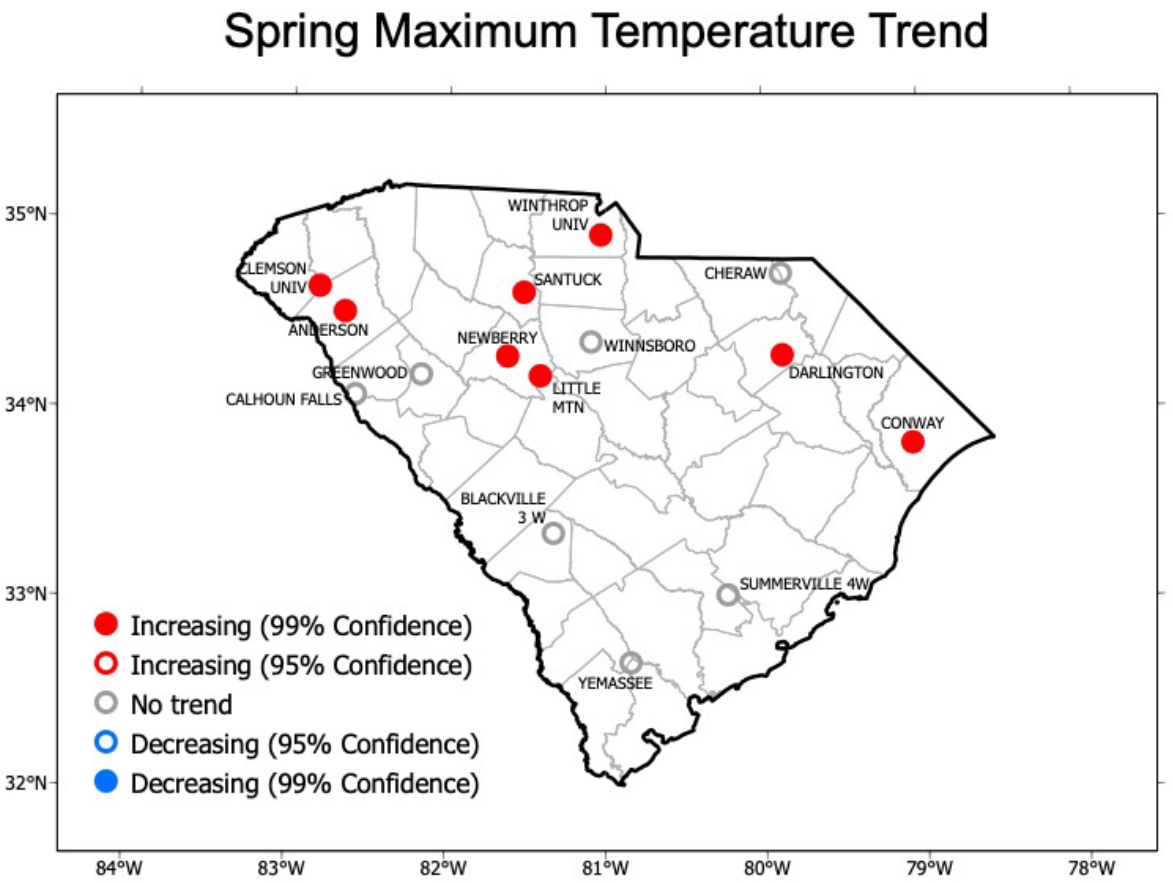


*Figure 5.5: Spring maximum temperature trend, 1900-2020.*

ALT / Screenreader text: This figure is a map showing stations in South Carolina that have experienced a statistically significant spring maximum temperature trend. Eight stations have an increasing temperature trend at the 99% confidence level; seven stations have no trend.

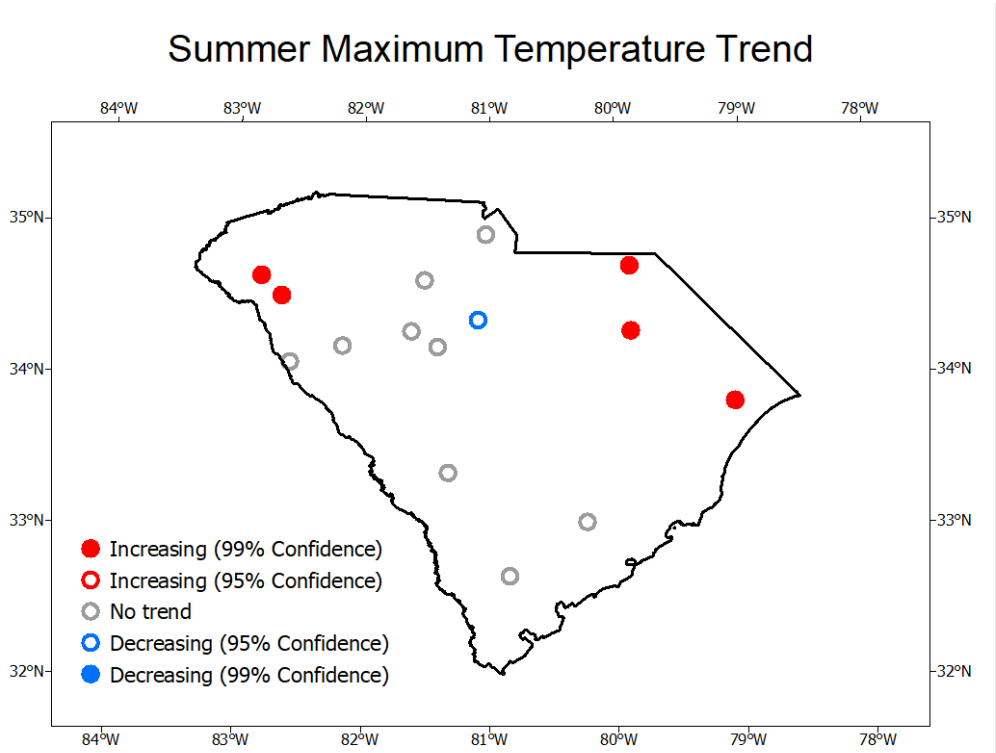


*Figure 5.6: Summer maximum temperature trend, 1900-2020*

ALT / Screenreader text: This figure is a map showing stations in South Carolina that have experienced a statistically significant summer maximum temperature trend. Five stations have an increasing temperature trend at the 99% confidence level; one station has a decreasing trend at 95% confidence; nine stations have no trend.

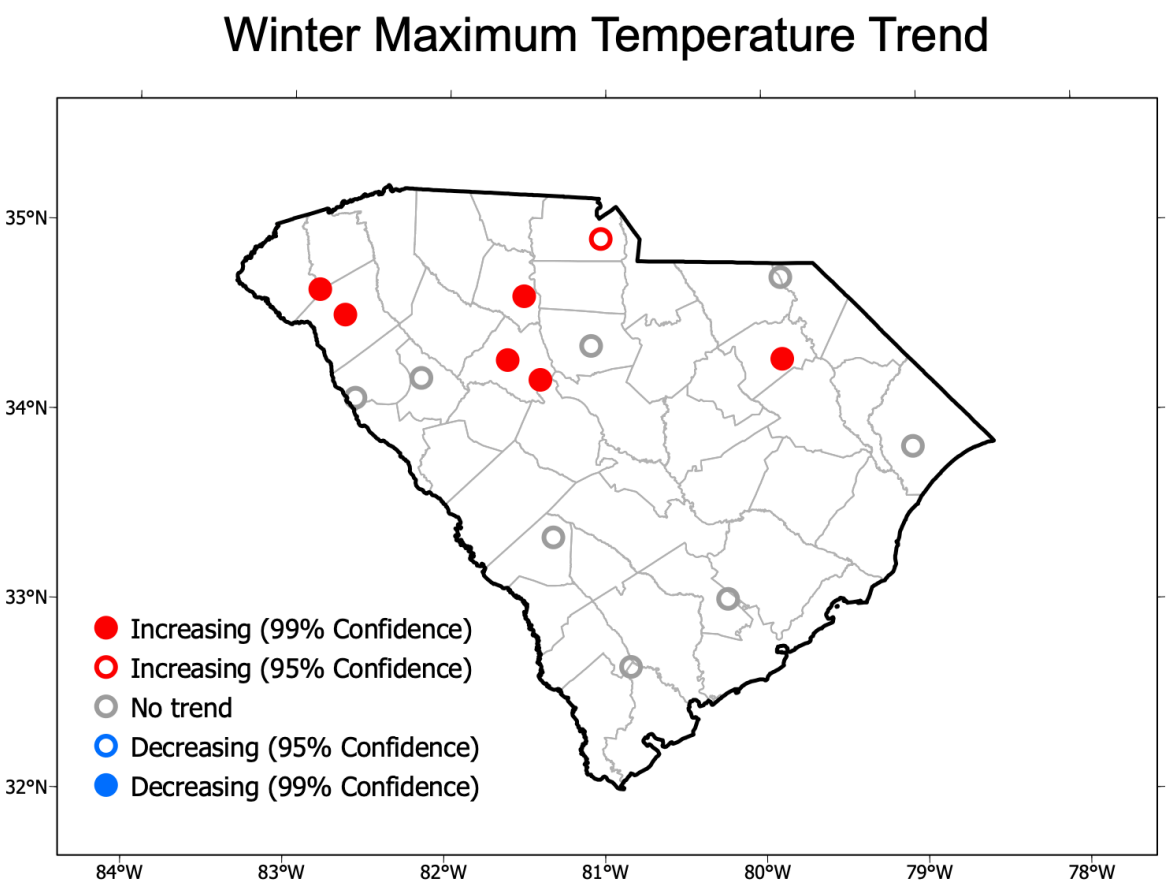


*Figure 5.7: : Winter maximum temperature trend, 1900-2020*

Screenreader text: This figure is a map showing stations in South Carolina that have experienced a statistically significant winter maximum temperature trend. Six stations have an increasing temperature trend at the 99% confidence level; one station has an increasing trend at 95% confidence; eight stations have no trend.

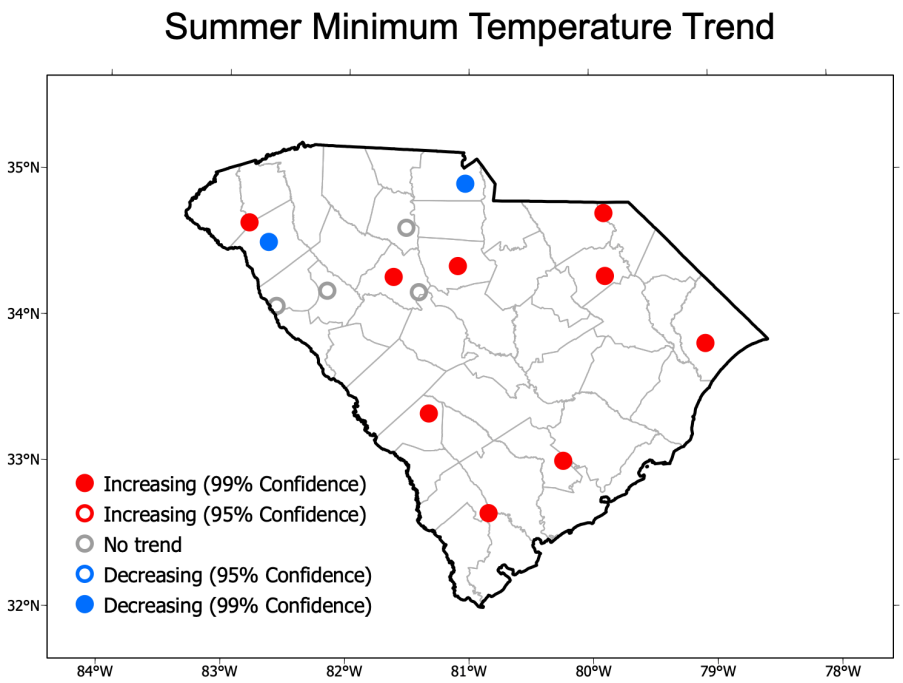


*Figure 5.8: Summer minimum temperature trend, 1900-2020*

ALT / Screenreader text: This figure is a map showing stations in South Carolina that have experienced a statistically significant summer minimum temperature trend. Nine stations have an increasing temperature trend at the 99% confidence level; two stations have a decreasing trend at 99% confidence; four stations have no trend.

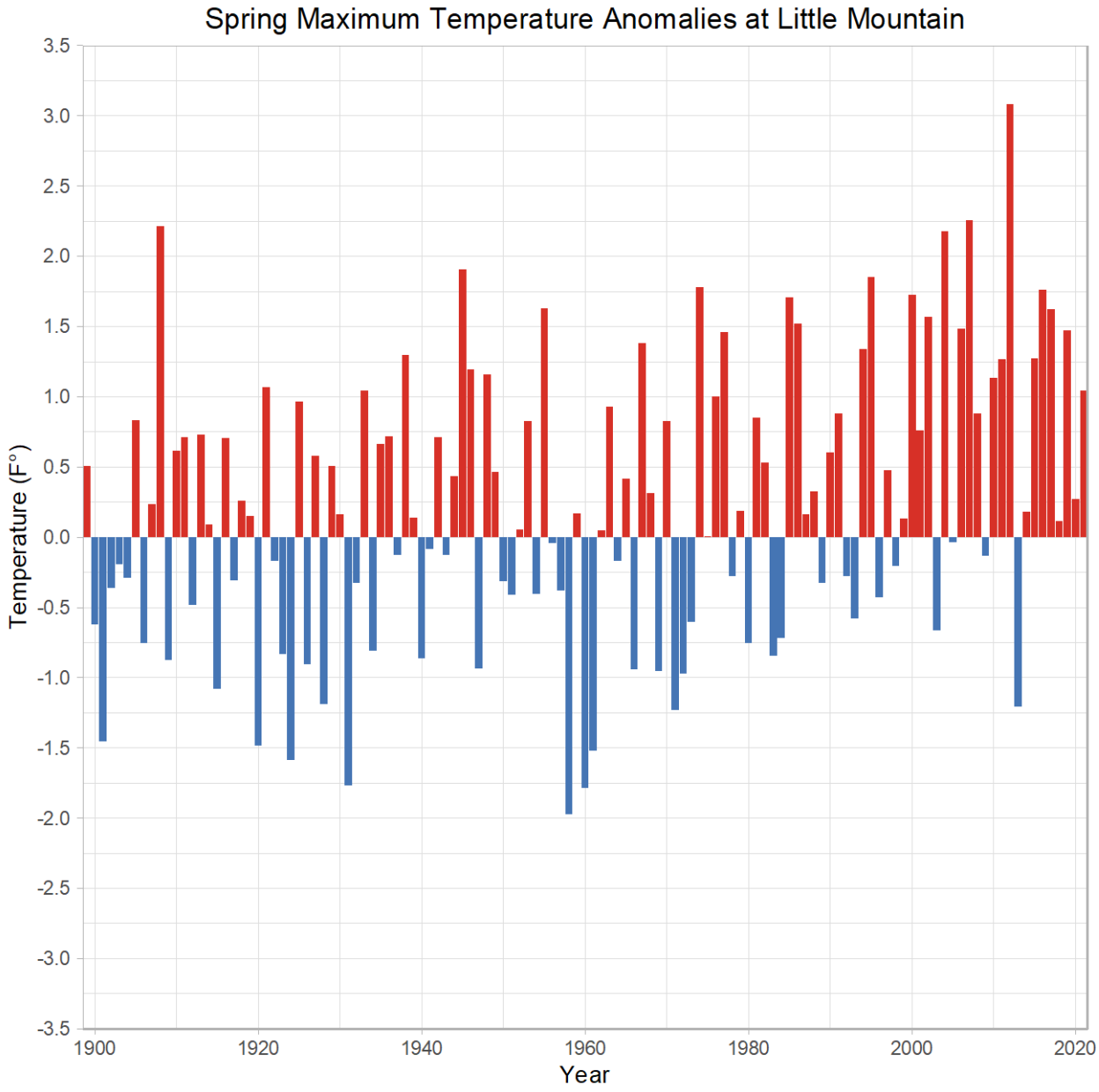


*Figure 5.9: 1900-2020 Little Mountain, South Carolina Spring maximum temperature anomalies (from 1900-1960 average)*

ALT / Screenreader text: This figure is a bar graph of spring maximum temperature anomalies at Little Mountain, South Carolina. The x-axis shows years from 1900 to 2020; the y-axis shows temperature anomaly from the 1900 to 1960 average, ranging from -3.5 to 3.5. From 1900 to around 1980, cool anomalies are as numerous as warm anomalies . From 1980 to 2020, there are noticeably fewer years with cold anomalies.

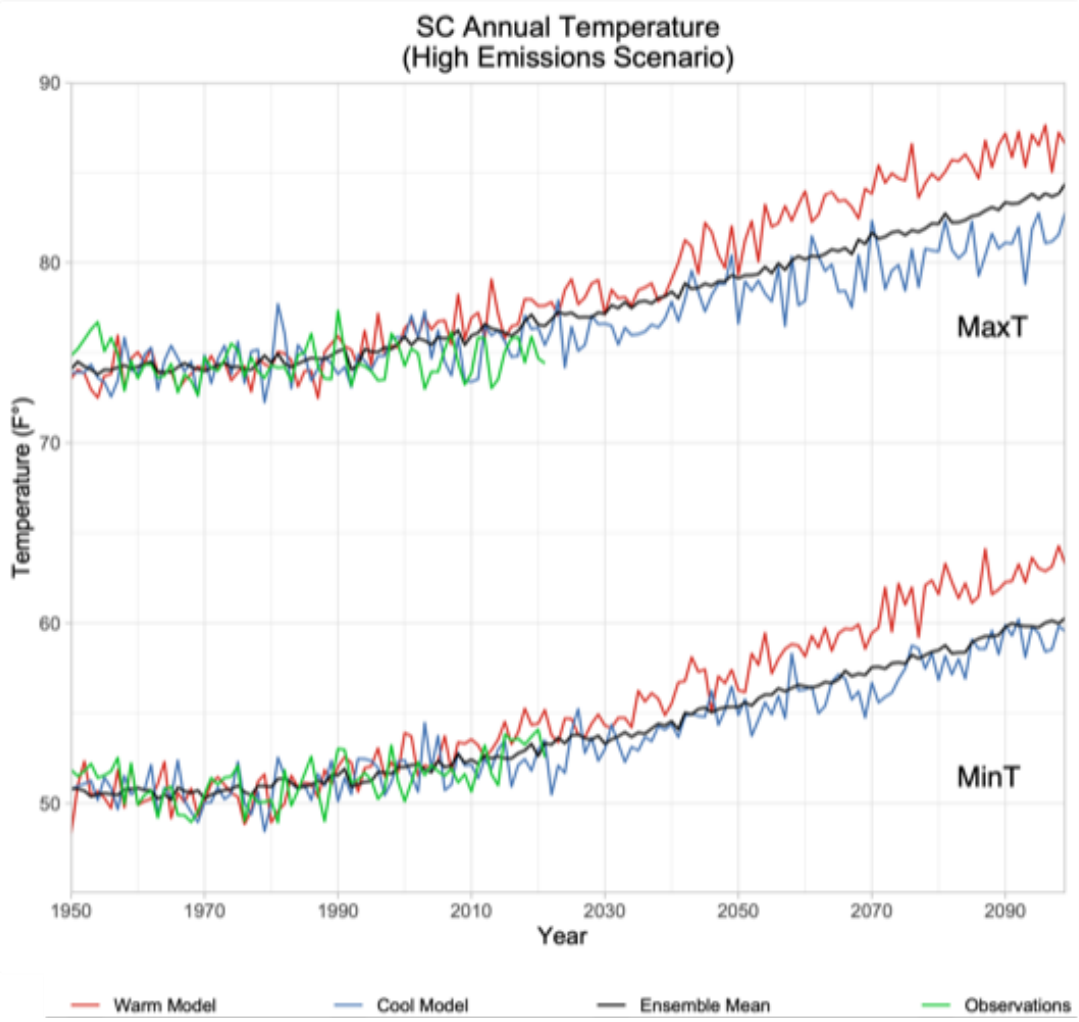


*Figure 5.10: Modeled vs. observed annual, state-averaged maximum and minimum temperature*

ALT / Screenreader text: This figure shows years ranging from 1950-2100 on the x-axis and temperature ranging from 45 to 90 degrees Fahrenheit on the y-axis. There are two sets of lines, one for maximum temperature and one for minimum temperature. Within each set, one line shows observed temperature from 1950 to 2020 and climate model temperature from 1950 to 2100 for: a warm model, a cool model, and an ensemble mean. Both maximum and minimum simulated temperature increases through time, especially after 2000. The models closely follow observed data during the overlapping, 1950-2020 period.

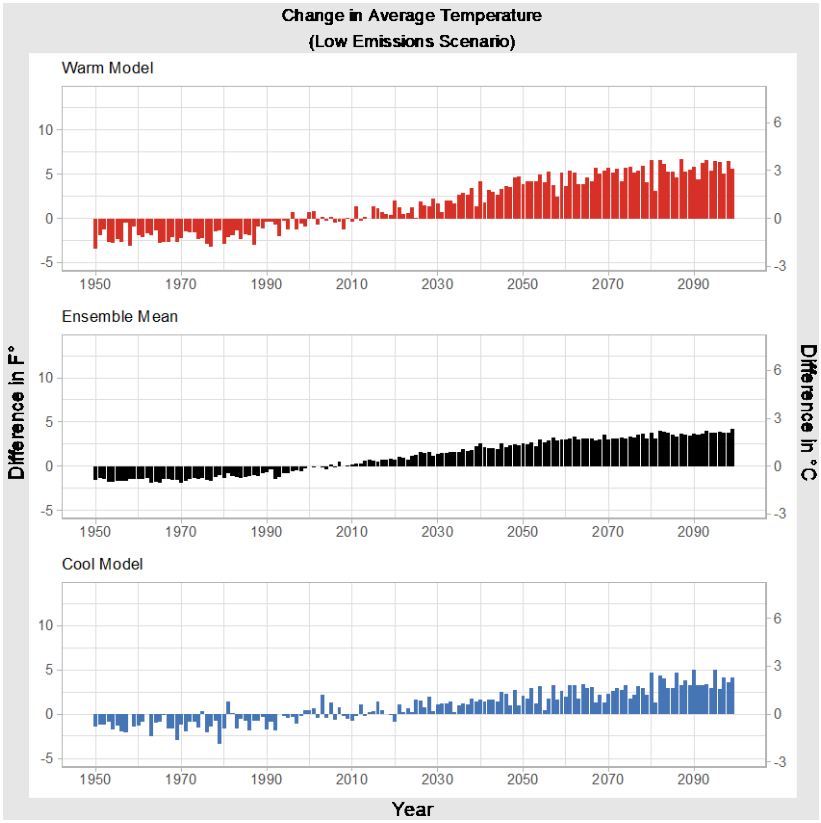


*Figure 5.11: Model simulated average temperature for South Carolina. Projections are measured as departures (anomalies) from the 1991-2020 mean (RCP 4.5 emissions scenario).*

ALT / Screenreader text: This figure is a set of bar graphs showing projected average temperature change in South Carolina for a low emissions scenario (RCP 4.5) using three climate models: a warm model, a cool model, and the ensemble mean. The x-axis shows years ranging from 1950 to 2100, and the y-axis is difference in temperature from the 1991 to 2020 average in degrees Fahrenheit, ranging from -5 to 10 (an alternative axis in degrees Celsius is also shown). Each climate model shows the same noticeable visual trends. The first trend is an increase over time. The second trend is a switch around the year 2000, where the bars cross from showing a negative anomaly to showing positive anomalies after 2000. There are no negative anomalies in any model after 2020.

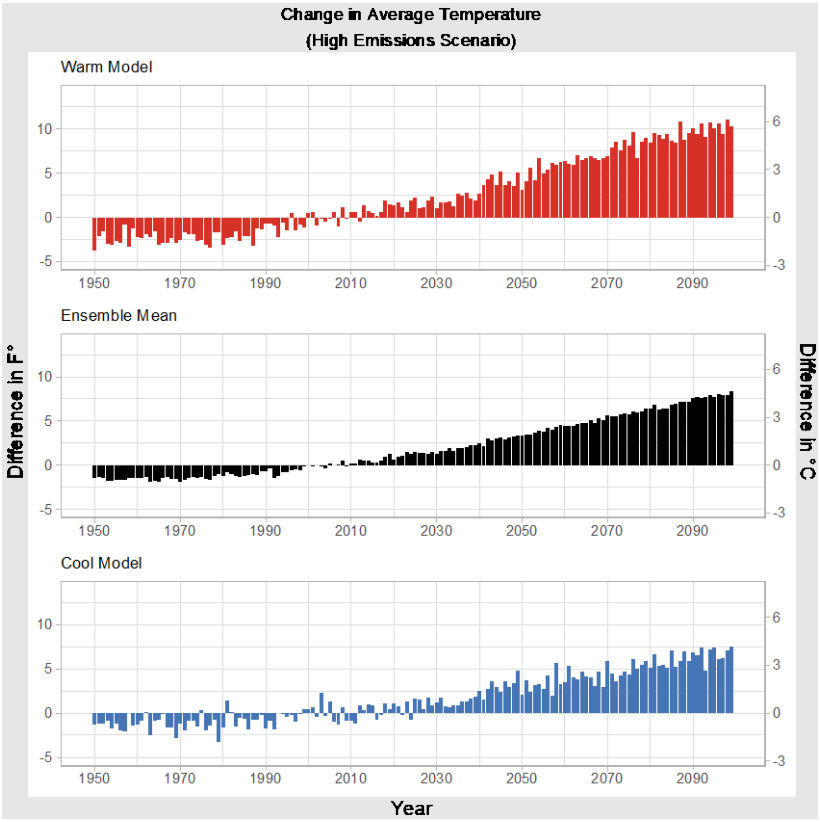


*Figure 5.12: Same as Figure 5.11, but for the high emissions scenario (RCP 8.5).*

ALT / Screenreader text: This figure is a set of bar graphs showing projected average temperature change in South Carolina for a high emissions scenario (RCP 8.5) using three climate models: a warm model, a cool model, and the ensemble mean. The x-axis shows years ranging from 1950 to 2100, and the y-axis is difference in temperature from the 1991 to 2020 average in degrees Fahrenheit, ranging from -5 to 10 (an alternative axis in degrees Celsius is also shown). Each climate model shows the same noticeable visual trends. The first trend is an increase over time. The second trend is a switch around the year 2000, where the bars cross from showing a negative anomaly to showing positive anomalies after 2000. There are no negative anomalies in any model after 2030.

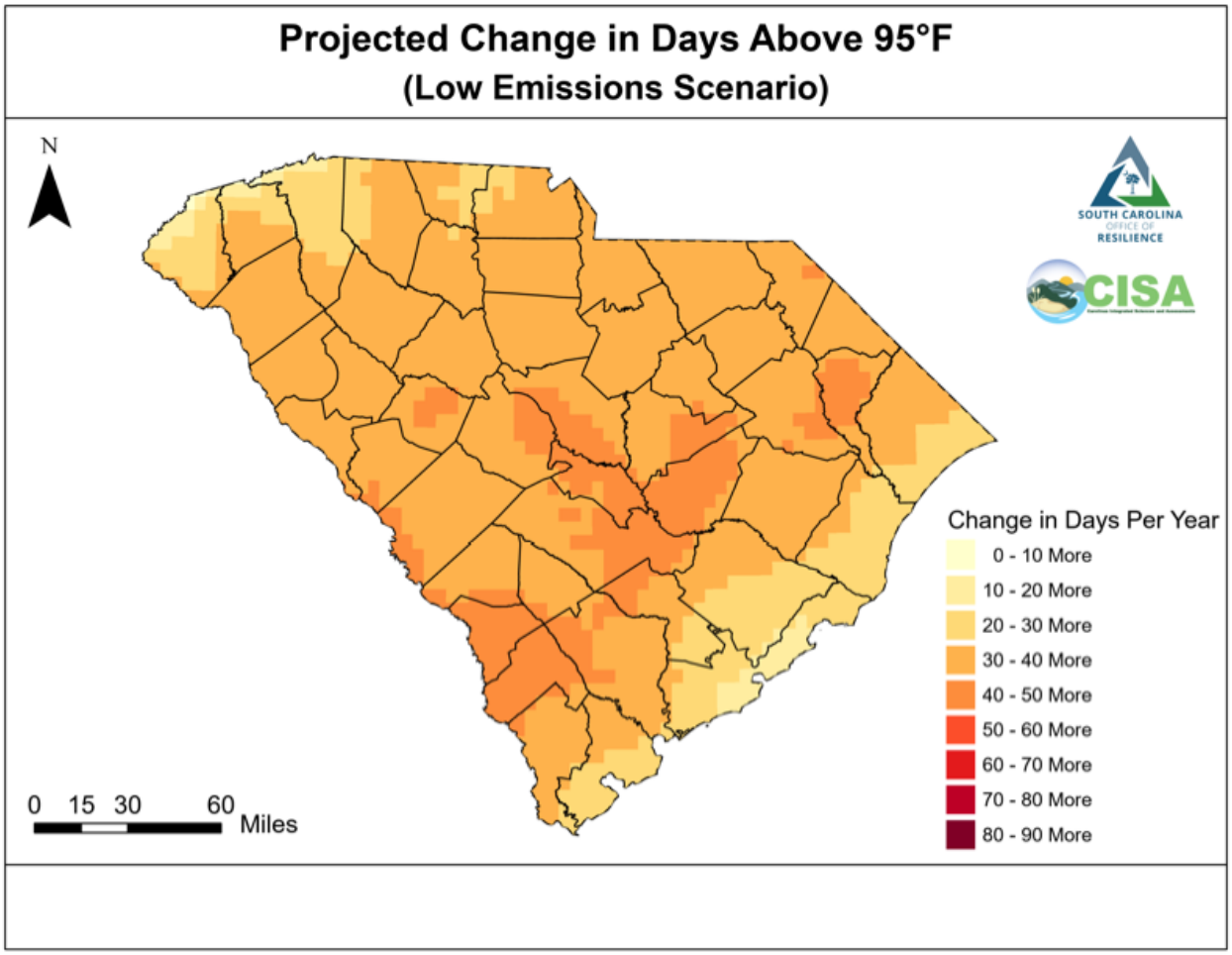


*Figure 5.13: Projected increase in the number of days per year with maximum temperature above 95°F (RCP 4.5 emissions scenario).*

ALT / Screenreader text: This figure is a map of South Carolina showing the change in number of days per year with a maximum temperature higher than 95 degrees Fahrenheit for the lower emissions scenario (RCP 4.5) as projected by an average of nine climate models. All parts of the state have an increase in such days ranging from 0 to 20 more days near the coast and in the mountains, 30-plus more days across most of the rest of the state, and 40-50 more days in the inner coastal plain, across important agricultural areas of the state.

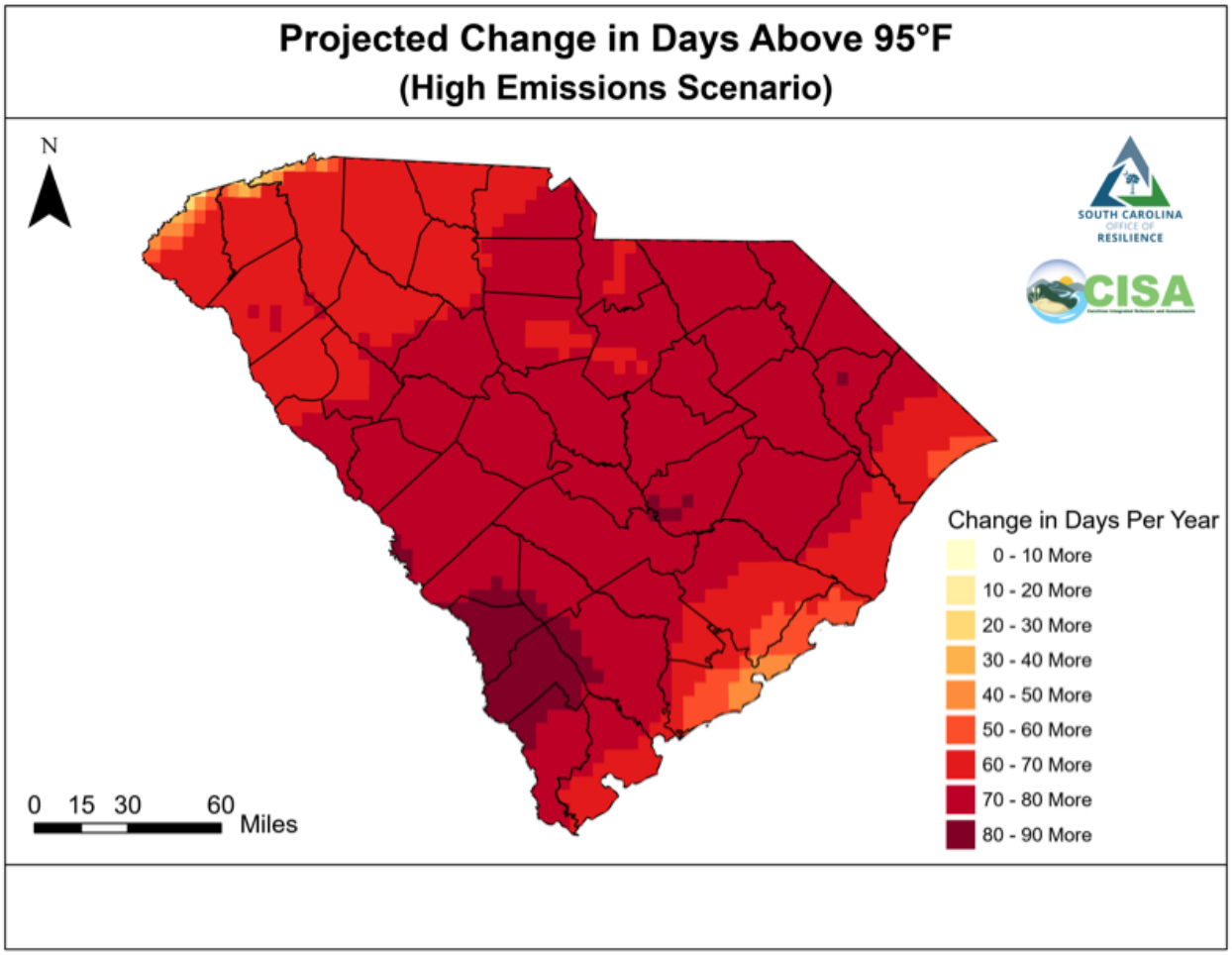


*Figure 5.14: Projected increase in the number of days per year with maximum temperature above 95°F (RCP 8.5 emissions scenario)*

ALT / Screenreader text: This figure is a map of South Carolina showing the change in number of days per year with a maximum temperature higher than 95 degrees Fahrenheit for the higher emissions scenario (RCP 8.5) as projected by an average of nine climate models. Nearly the entire state has at least 50 more days. More than half the state, from the outer coastal plain, through the Piedmont have at least 60 more days; some southern parts of the state have 80-90 more days.

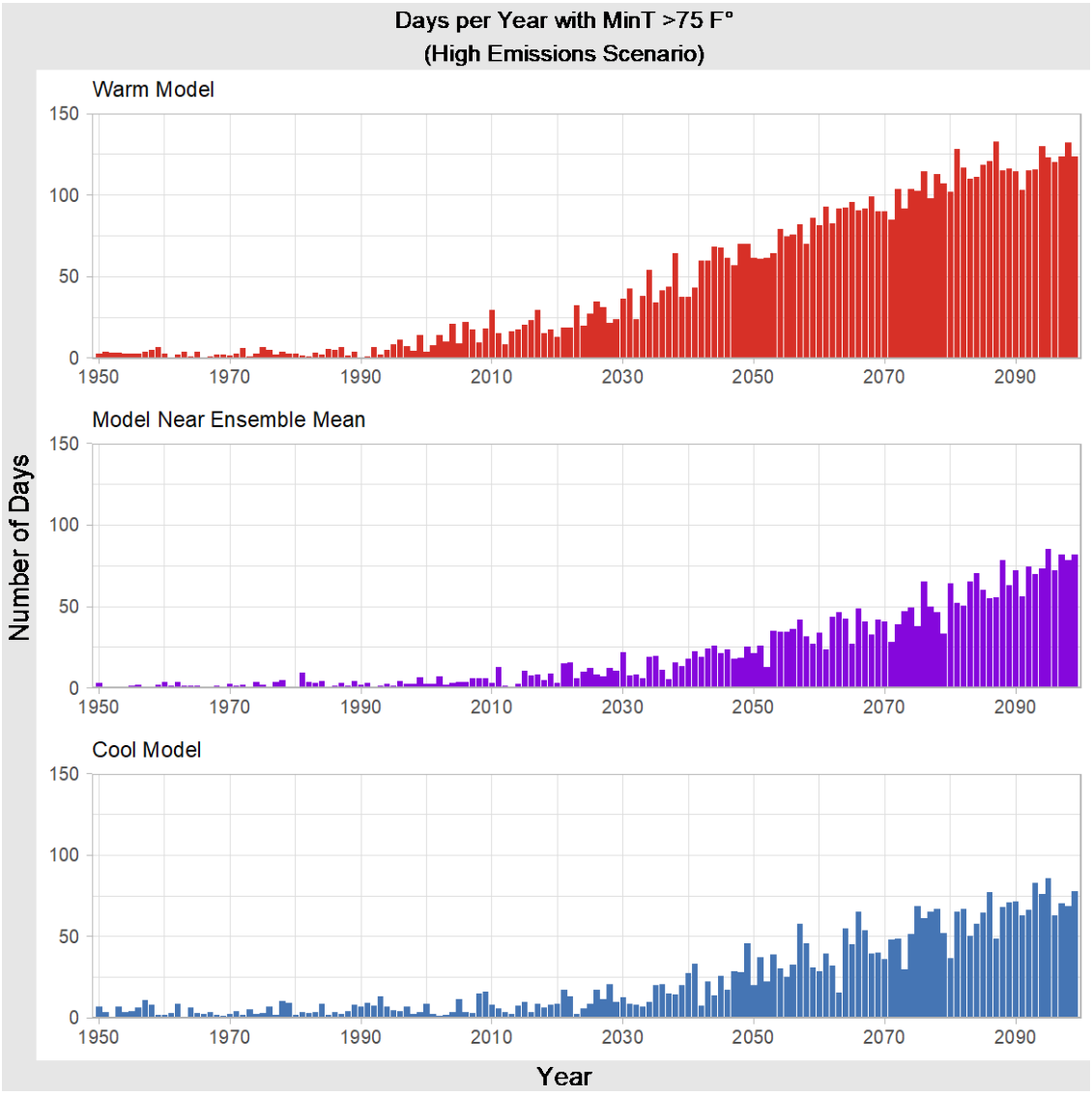


*Figure 5.15: Projected number of days per year with maximum temperature above 75°F (RCP 8.5 emissions scenario).*

ALT / Screenreader text: This figure is a set of bar graphs showing change in number of days per year with a minimum temperature higher than 75 degrees Fahrenheit for a low emissions scenario (RCP 4.5) using three climate models: a warm model, a cool model, an ensemble mean. The x-axis shows years from 1950 to 2100; the y-axis shows number of days ranging from zero to 150. All models show a noticeable increase in the number of days as time progresses.

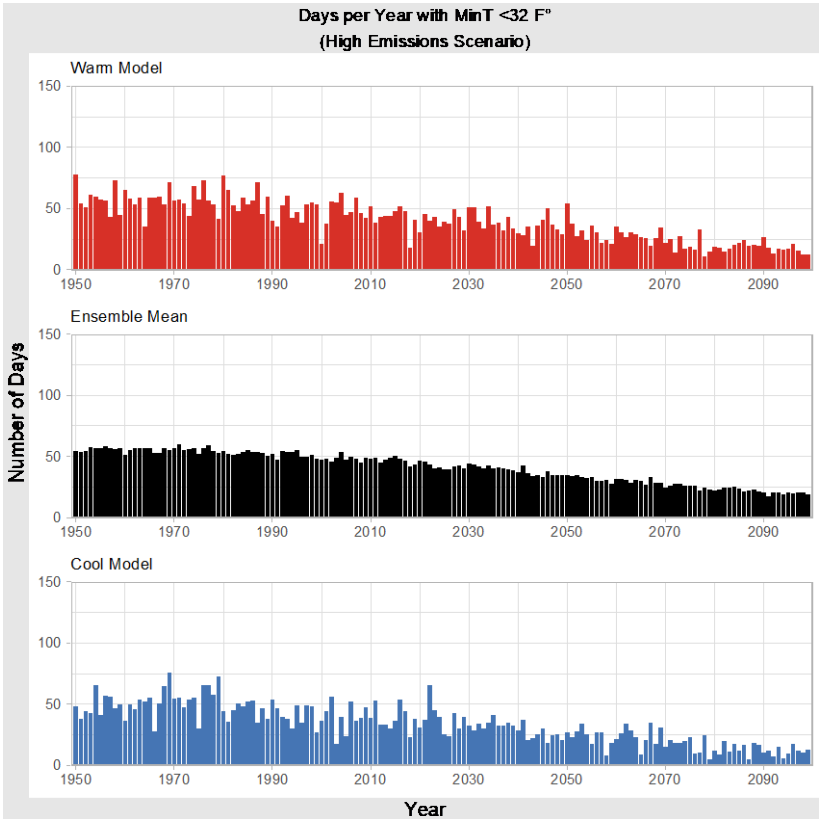


*Figure 5.16: Projected number of days per year with minimum temperature below 32°F (RCP 8.5 emissions scenario).*

ALT / Screenreader text: This figure is a set of bar graphs showing change in number of days per year with a minimum temperature below 32 degrees Fahrenheit for a high emissions scenario (RCP 8.5) using three climate models: a warm model, a cool model, an ensemble mean. The x-axis shows years from 1950 to 2100; the y-axis shows number of days ranging from zero to 150. All models show a noticeable decrease in the number of days as time progresses, especially after around 2070.

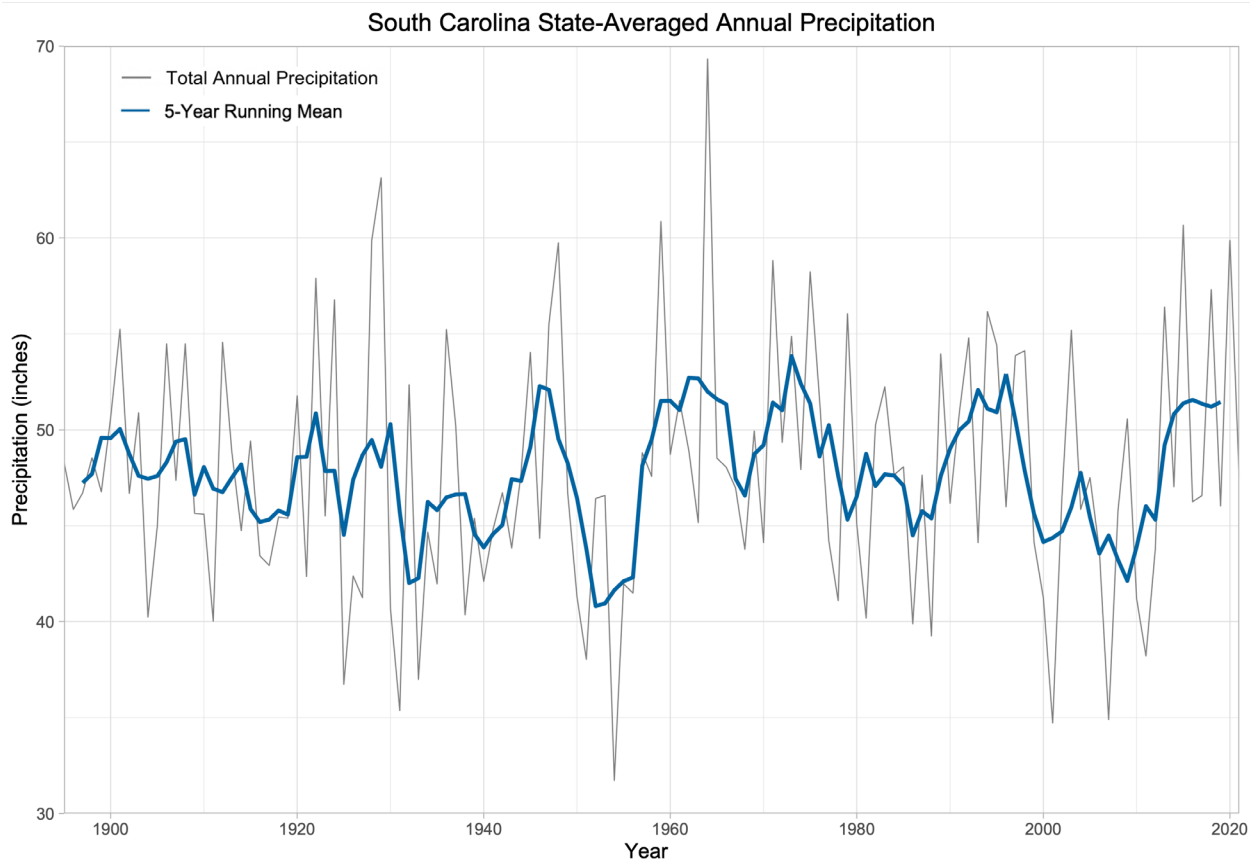


*Figure 5.17: State-averaged total annual precipitation.*

ALT / Screenreader text: This figure is a line graph showing South Carolina's state-averaged annual precipitation; one line shows annual precipitation, and a second line shows a 5-year running mean. The x-axis shows years from 1900 to 2020; the y-axis shows precipitation ranging from 30 to 70 inches. The graph shows a lot of interannual variability without a clear trend.

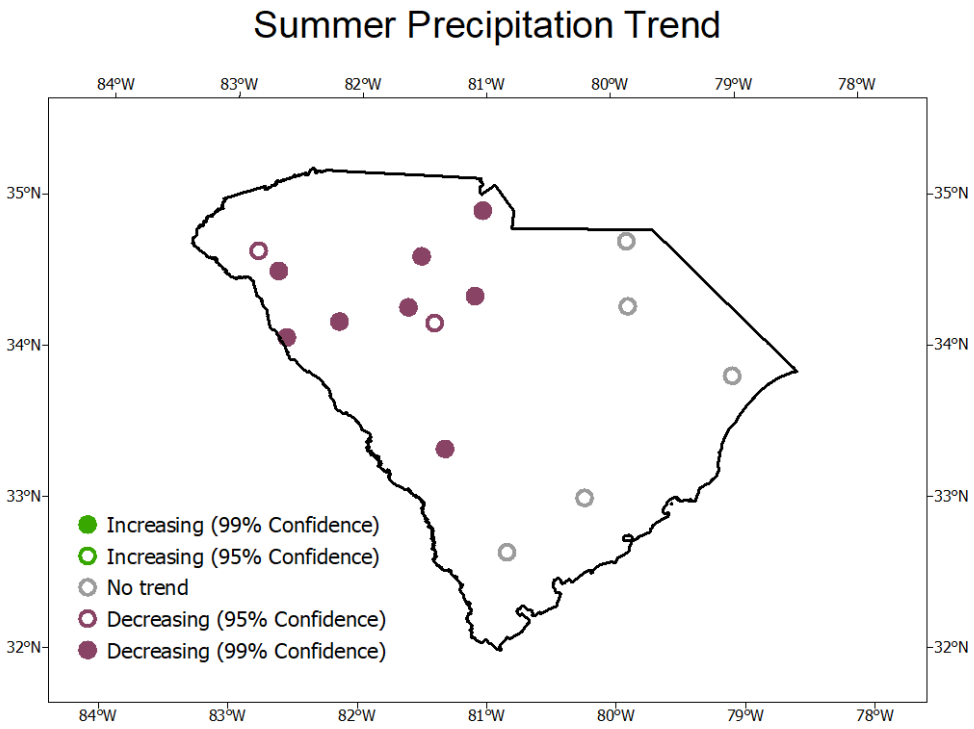


*Figure 5.18: Summer precipitation trend, 1900-2020.*

ALT / Screenreader text: This figure is a map showing summer precipitation trends at 15 long-term South Carolina stations. 8 stations show a statistically significant decrease at 99% confidence; 2 stations are decreasing at 95% confidence, and 5 stations show no trend.

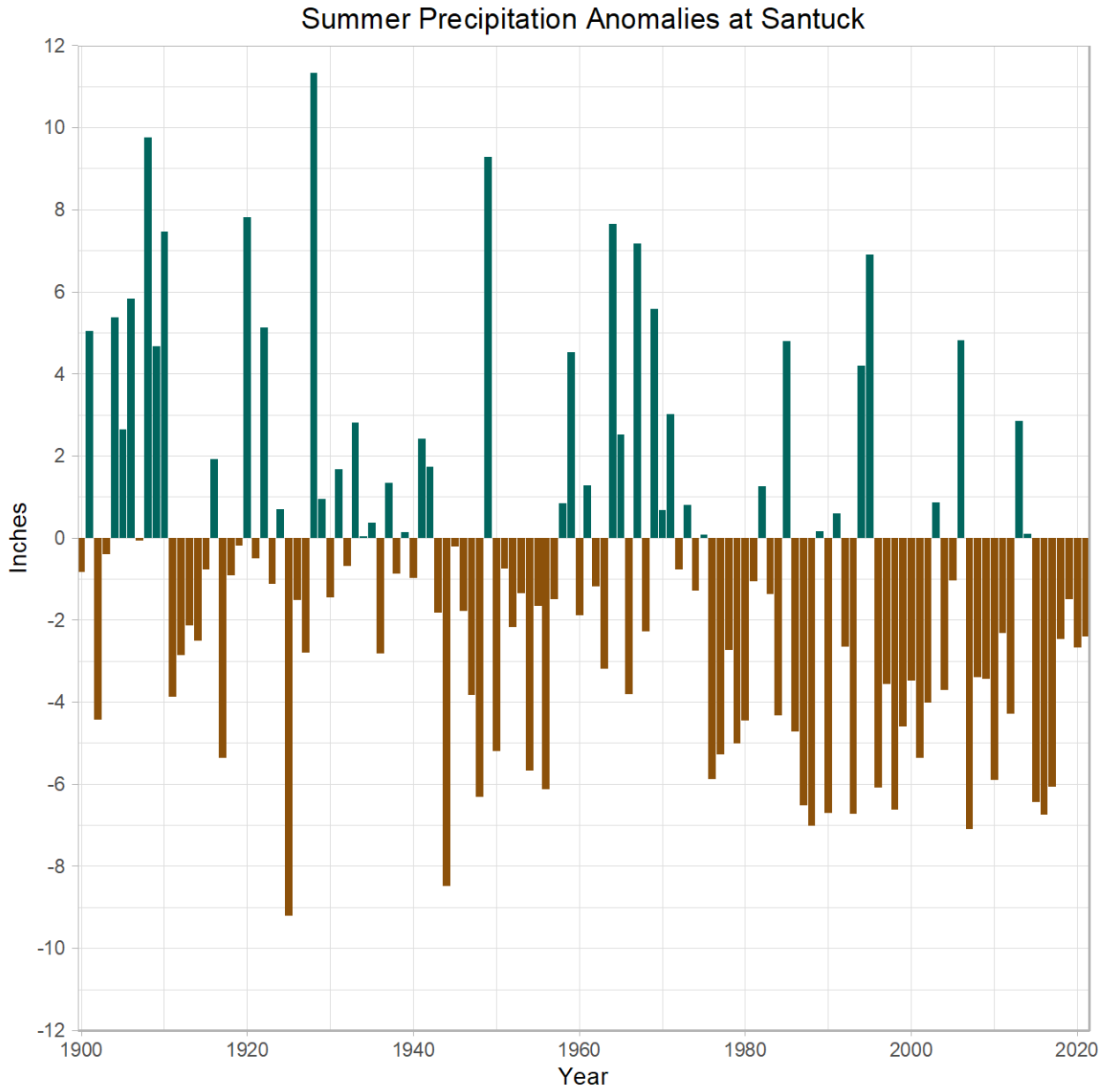


*Figure 5.19: Santuck, SC summer precipitation anomalies from 1901-1960 mean.*

ALT / Screenreader text: This figure is a bar graph showing summer precipitation anomalies at Santuck. The x-axis shows years from 1900 to 2020; the y-axis shows precipitation anomalies from the 1900 to 1960 average, ranging from -12 to +12 inches. The graph shows a lot of interannual variability without a clear trend.

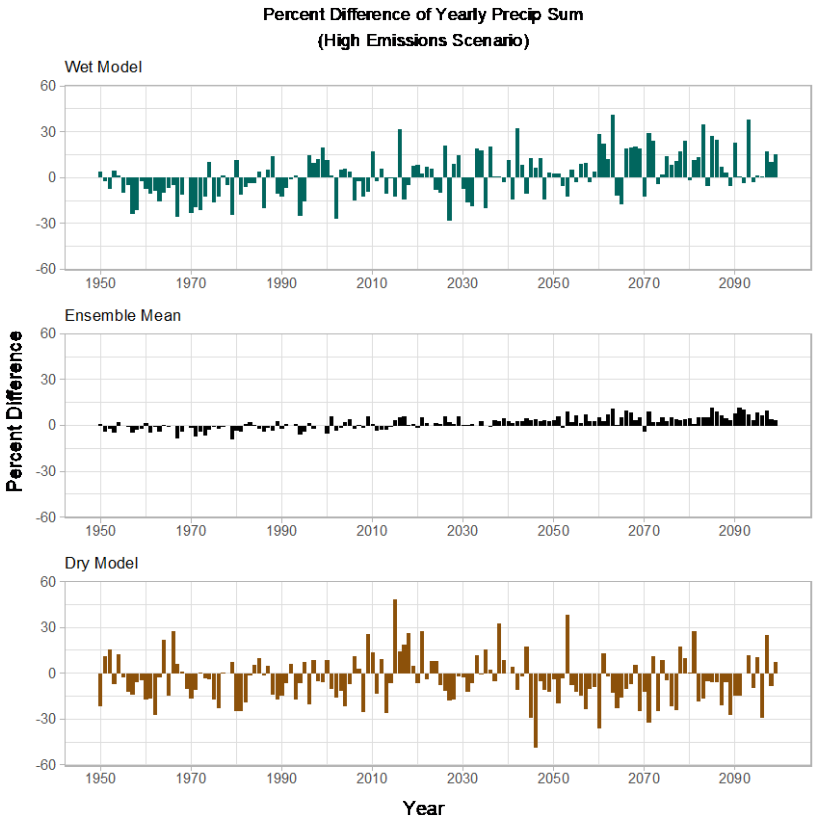


*Figure 5.20: Model projected annual precipitation as percentage greater or less than 1991-2020 mean.*

ALT / Screenreader text: This figure is a set of bar graphs showing projected annual precipitation relative to the 1991-2020 average for a low emissions scenario (RCP 4.5) using three climate models: a wet model, a dry model, and the ensemble mean. The x-axis shows years ranging from 1950 to 2100, and the y-axis is percentage annual precipitation relative to the 1991 to 2020 average, ranging from -60% to +60%. Most notably, the wet model shows late 21st century annual precipitation values that range between 5 and 30% higher than the current average. The dry model shows late 21st century annual precipitation values that range between 5 and 30% lower than the current average. The ensemble average shows slight values between 1 and 10% higher than the current average.

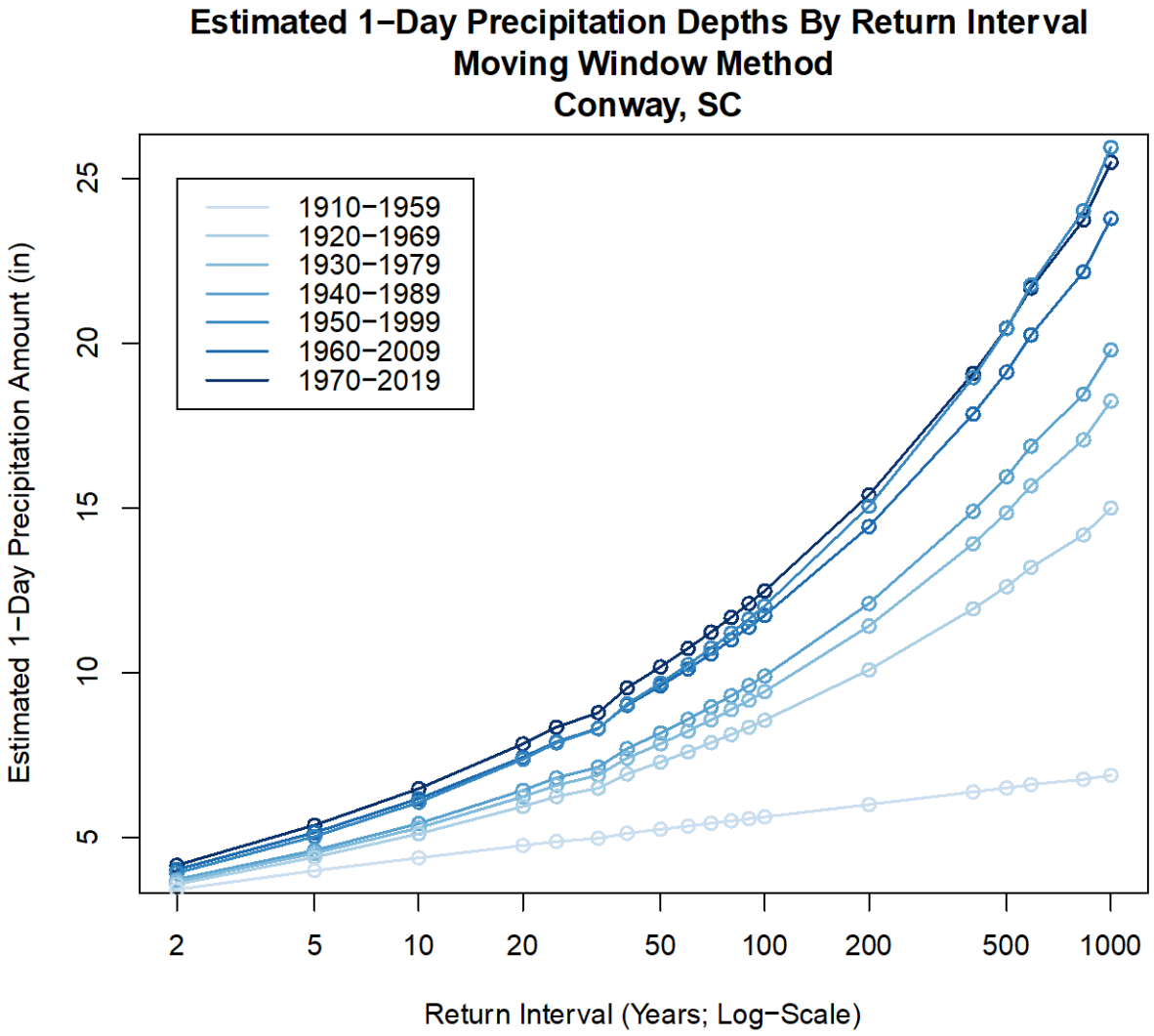


*Figure 5.21: Average recurrence interval of 1-day precipitation depths calculated for separate 50-year periods. Shading is lightest for earliest period (1910-1959) and darkest for most recent period (1970-2019).*

ALT / Screenreader text: This figure shows the probability (shown on the x-axis) associated with a given 1-day precipitation depth (shown on the y-axis). Probability is expressed as a return interval, precipitation depth is expressed in inches. Seven probability curves are shown, each for a 50-year period. The first period runs from 1910 to 1959, the next runs from 1920 to 1969, the seventh curve represents the period 1970 to 2019. The curves collectively show relatively low probability of a given precipitation depth in the earliest 50 years (1910-1959) compared to recent decades. These probabilities increase for the 50-year blocks that begin in 1920, 1930, and 1940, then jump again and are clustered for 50-year blocks that begin in 1950, 1960, and 1970 (all of which include heavy precipitation associated with Hurricane Floyd in 1999.

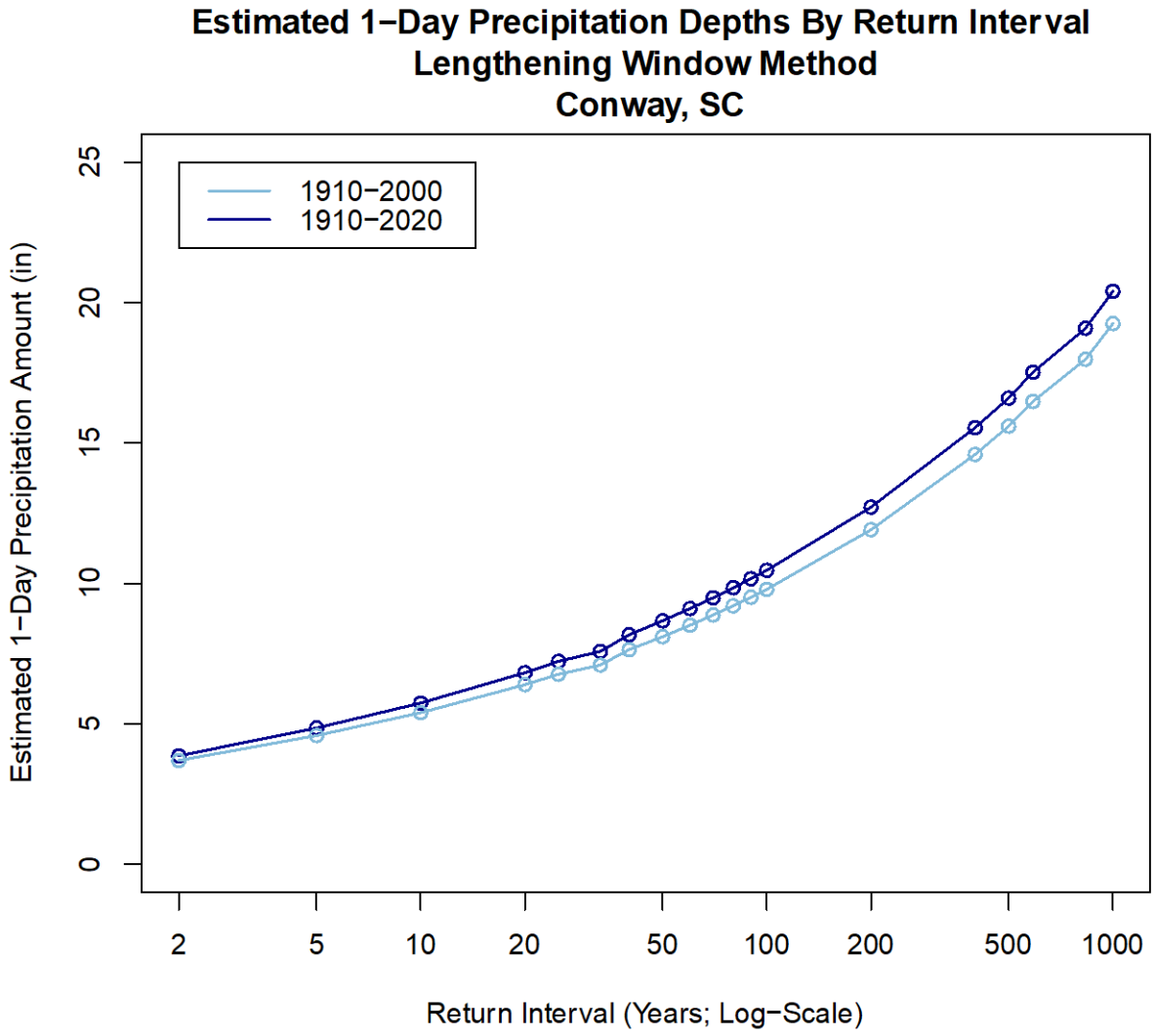


*Figure 5.22*: Average recurrence interval of 1-day precipitation depths calculated separately for 1910-2000, and for 1910-2020.

ALT / Screenreader text: This figure shows the probability (shown on the x-axis) associated with a given 1-day precipitation depth (shown on the y-axis). Probability is expressed as a return interval, precipitation depth is expressed in inches. Two probability curves are shown, one for the period 1910 to 2000, the other for the period, 1910-2020. The curves are very similar, indicating that adding the most recent 20 years makes little difference to the probability associated with a given 1-day precipitation event. This is largely because both time series include heavy precipitation associated with Hurricane Floyd in 1999, and subsequent storms have approached, but have not exceeded this value.

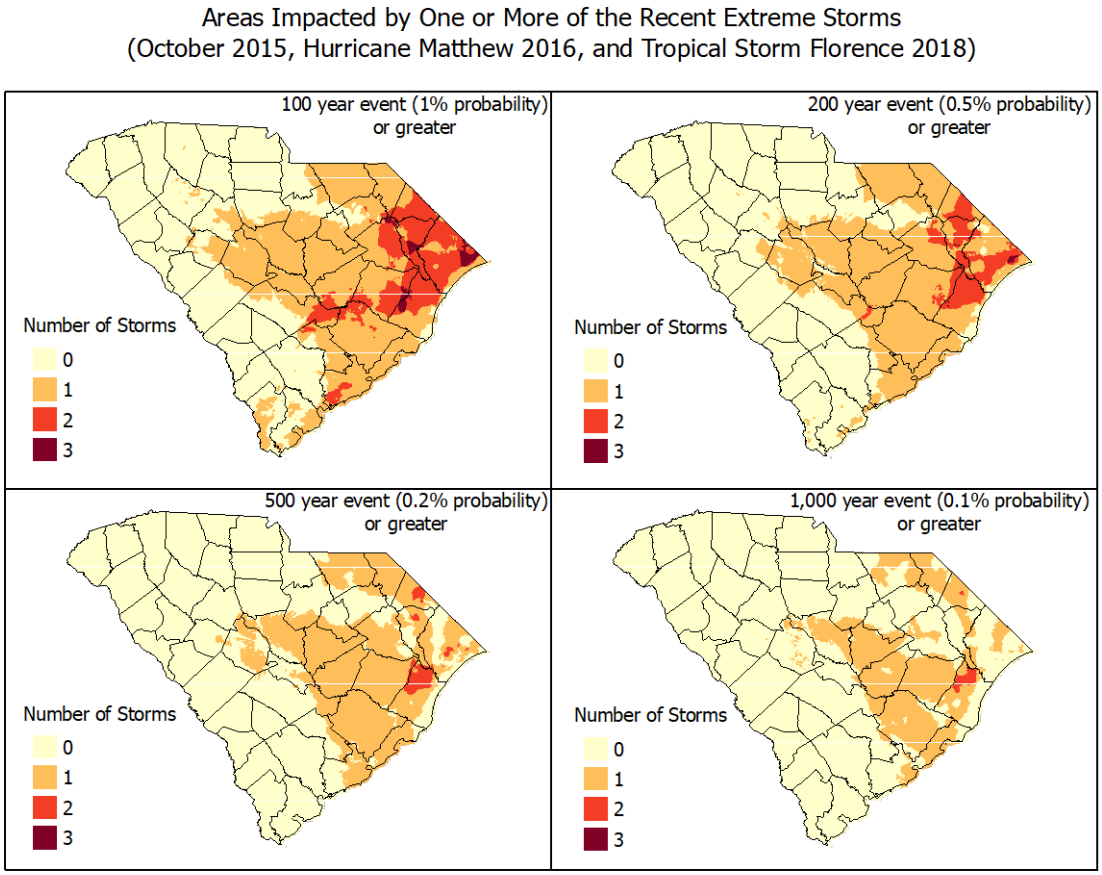


*Figure 5.23: Areas experiencing 100-, 200-, 500-, and 1000-year rainfall events due to one or more of the recent extreme storms. (Data provided by SC Department of Natural Resources.)*

ALT / Screenreader text: This figure includes 4 maps showing areas of South Carolina affected by the October 2015 flood event, Hurricane Matthew in 2016, and Tropical Storm Florence in 2018. Areas are shaded indicating the number of these storms (0 to 3) that caused a 100-year, 200-year, 500-year, or 1,000-year event. The maps show that half the state, specifically areas in the Midlands, Coastal Zone, and northeastern portions of the state experienced at least one 100-year event, and approximately a third of the state experienced at least one 500-year event. Scattered coastal areas (totaling the equivalent of several counties) experienced two 100-year events; the northeast corner of the state had scattered areas (about two counties worth) that experienced two 200-year events. Other isolated areas in river flood plains (totaling the equivalent of one small county) experienced three 100-year events in this short period. ..

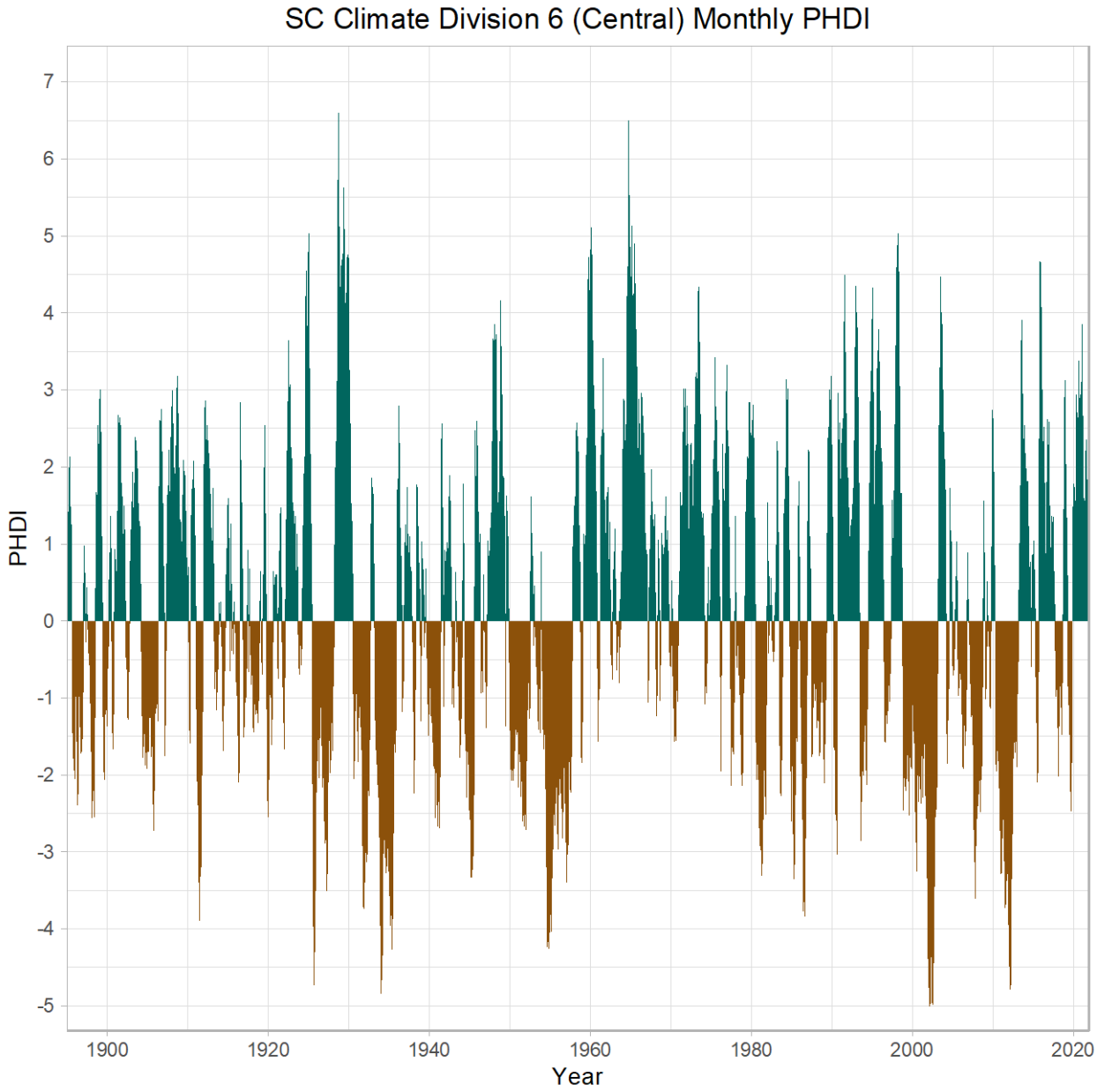


*Figure 5.24: Palmer Hydrological Drought Index 1895-2020.*

ALT / Screenreader text: This figure is a filled-line graph showing a time series of the Palmer Hydrological Drought Index for South Carolina Climate Division 6 at monthly intervals. The x-axis shows year from 1895– 2020, and the y-axis shows the index values ranging from –5 to 7. The graph shows a lot of interannual variability without a clear trend.

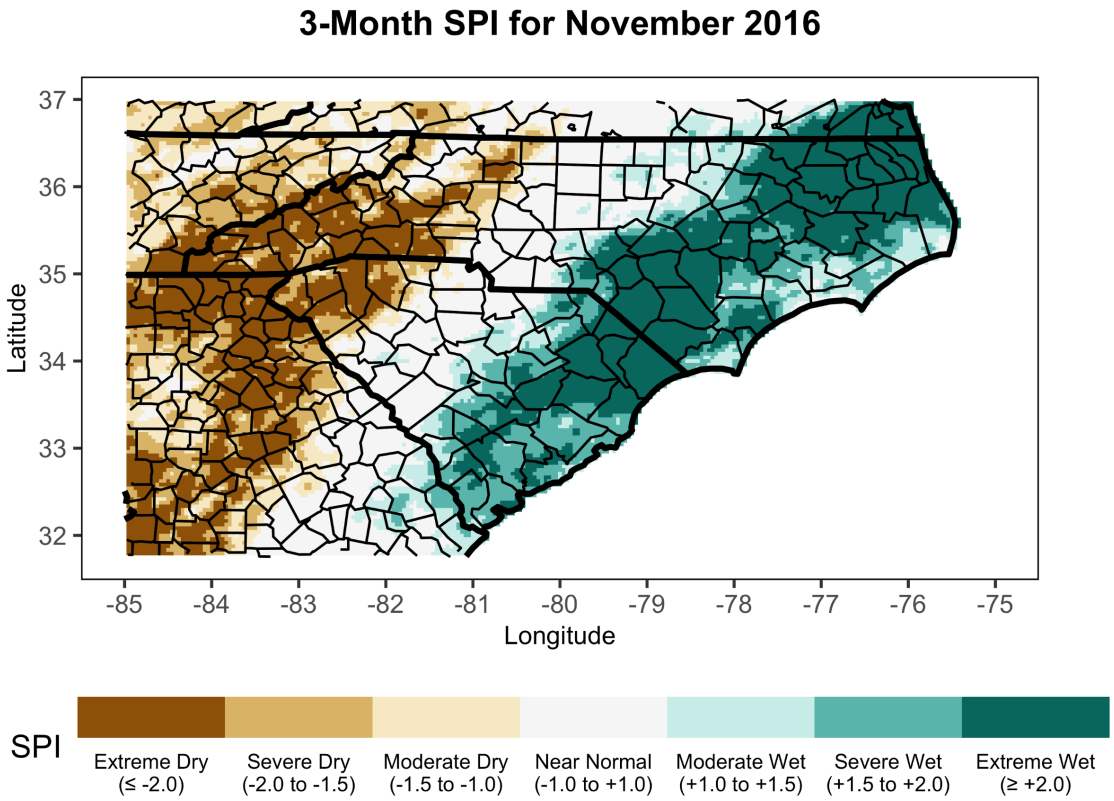


*Figure 5.25: Variability of Drought across South Carolina (Fall 2016)*

ALT / Screenreader text: This figure is a map showing the 3-month standardized precipitation index for November 2016 across North Carolina and South Carolina. The legend shows areas of the index that indicate dry or wet conditions. The visual pattern is a swath of extremely dry areas in the Western regions of the Carolinas and a swath of extremely wet areas on the coastal plain of the Carolinas. In the area between these two swaths, conditions are near normal.

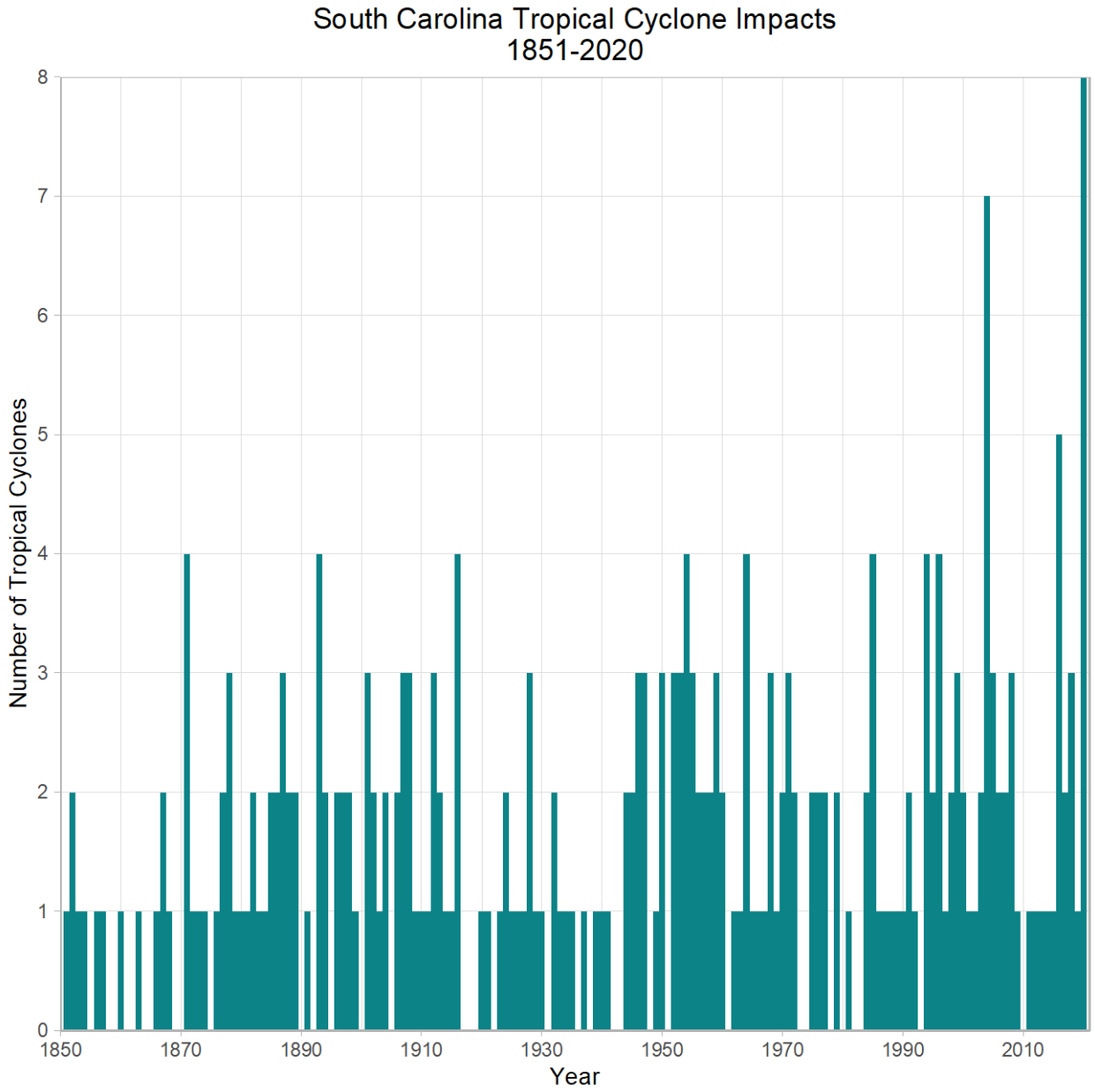


*Figure 5.26: Tropical Cyclones affecting South Carolina, 1851-2020.*

ALT / Screenreader text: This figure is a bar graph showing the number of tropical cyclone impacts in South Carolina for a given year. The x-axis shows years from 1850 to 2020, and the y-axis shows the number of storms ranging from 0 to 8. The graph shows a lot of interannual variability.

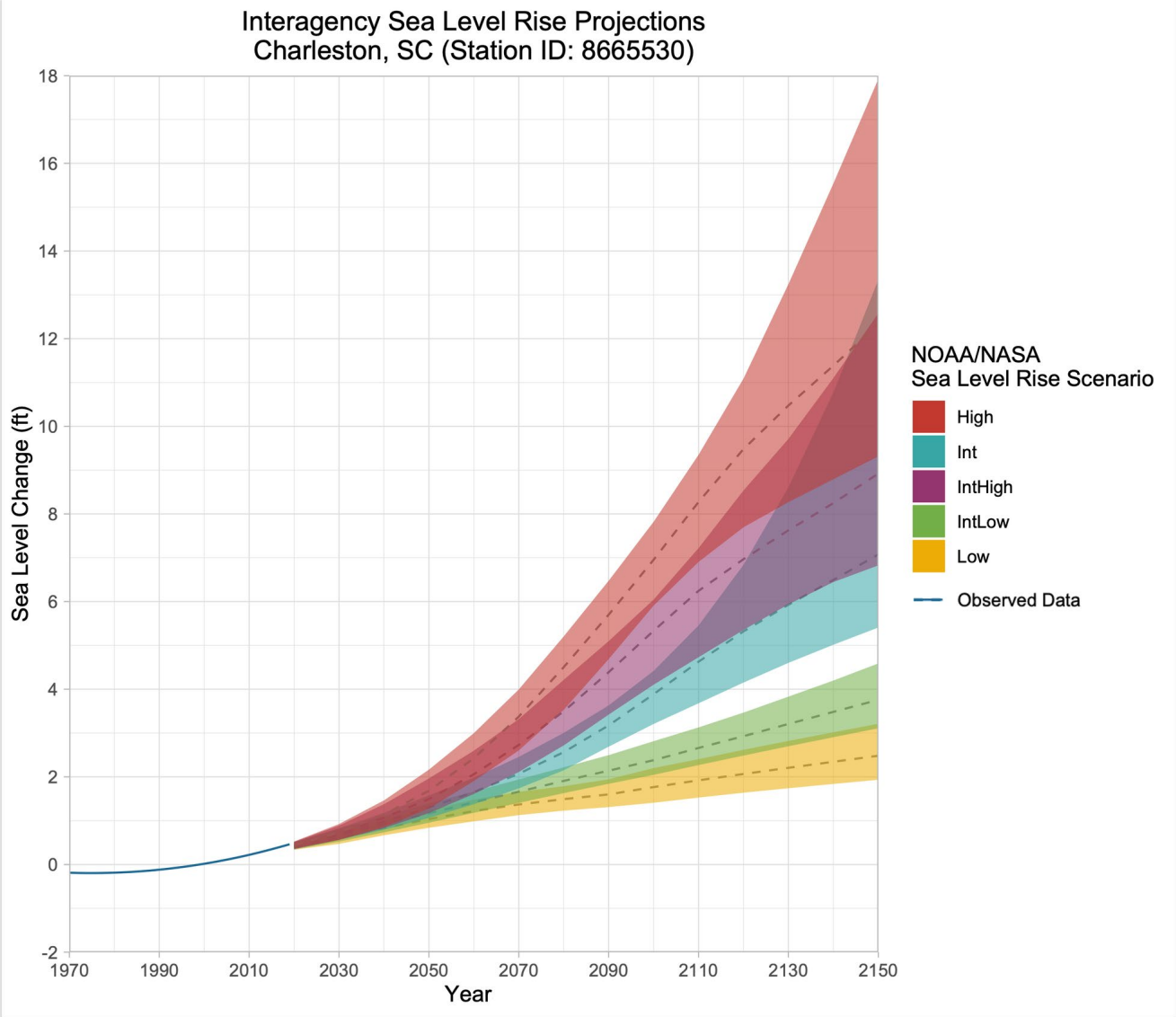


*Figure 5.27: Charleston sea level change projections (Adapted from Sweet et al., 2022).*

ALT / Screenreader text: This figure shows a line graph, with years on the x-axis and sea level change in feet on the y-axis. The line from 1970 to 2020 shows observed data, with an increase of about 0.75 feet during those years. From 2020 to 2150 shows diverging sea level rise scenarios as colored lines. The Low and Intermediate-Low scenarios show linear increases of 2-3 feet by 2150. The Intermediate, Intermediate-High, and High scenarios show exponential increases. By 2150, the Intermediate scenario shows a median of 7 feet, the Intermediate-High scenario shows a median of 9 feet, and the High scenario shows a median of 12 feet. The maximum point, the upper boundary of the High scenario, is near 18 feet by 2150.

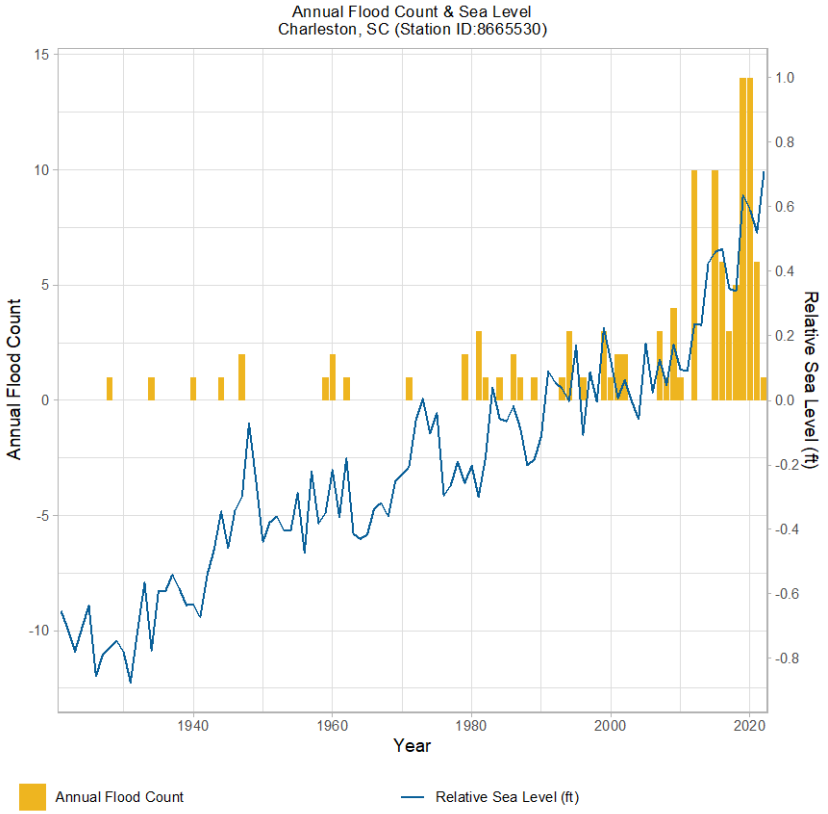


*Figure 5.28: Annual Flood Count and Sea Level at Charleston Gauge. Sea level is relative to the current National Tidal Datum Epoch, 1983-2001.*

ALT / Screenreader text: This figure shows two overlapping plots, relative sea level change in feet as a line graph and number of annual floods per year (defined as an event greater than or equal to 1.87 feet above MHHW) as a bar graph. The x-axis for both graphs is year, ranging from 1900 to 2021. The line graph of relative sea level change shows an increase of 1.1 foot across the past 100 years. The bar graph shows intermittent floods from 1900 to 2010. After 2010, the number of floods noticeably increases, with several years having more than 5 floods or 10 floods, whereas there were no such years prior to 2010. The increase in floods occurs about 5 years after the relative sea level trend crosses the boundary and becomes positive relative to the reference period (the current National Tidal Datum Epoch, 1983-2001).